

Viewing 1950s Color, Over 50 Years Later

Was “Never Twice the Same Color” Ever Once the Right Color?

1 Introduction

The over-all quality of the color rendition of early NTSC color TV was affected by many non-ideal factors. Nevertheless, amateurs, and experts alike, sometimes wax nostalgic about the impression received from early color shows. While it is not possible to recreate the exact control settings and other variable conditions of a particular early broadcast, it is possible to determine the quality of color reproduction possible with early cameras under ideal conditions. Measurements of the spectral response of early cameras made at the time of the demonstrations of compatible color TV development, plus measurements of vintage equipment that still exists were entered into a spreadsheet. In addition, the spectra of light sources and a standard color test chart were entered. Spreadsheet formulas were written to calculate both the ideal reproduction and the actual color response of these cameras. Additional programming was done to create an accurate reproduction on a modern computer display of how the surviving image orthicon NTSC camera and its precursors would have reproduced the test chart. Furthermore, approximate effects of these cameras on real scene images were simulated using the results of the spreadsheet programs in an image processing program.

2 Many Factors

Some of the factors involved in color reproduction during the days of the three-image orthicon cameras (various versions of the RCA TK-40 and TK-41) are:

- Polarization sensitivity of the color-splitting dichroic optics (the effect typically was noticed as green highlights on back-lit hair)
- Image orthicon setup/operating conditions (Image orthicon setup appears to have been as much art as science – the tube had a narrow optimum temperature range for operation, and many of the electrical and magnetic field adjustments affected each other);
- Camera video processing setup (black level and gamma correction) – Early cameras with all-tube circuits were typically warmed up for hours before critical adjustments were attempted; the last version of the TK-41 boasted

improved stability to reduce the necessary stabilization time

- Camera optics not adapted to light-quality change – the TK-41s had neutral density filters in the R,G and B paths to allow adjusting for illumination color temperature, and did not have a filter wheel for color-compensating filters. It was the practice in some studios to run all (incandescent) lighting at 70% on the dimmers, and then adjust up and down from there.
- Signal-to noise ratio (SNR) of the cameras – Despite the relatively low SNR of the image orthicon output compared to modern cameras, the video processing added even more noise. RCA made improvements over the years. Xavier University, Cincinnati, received hand-me-down cameras and gutted them and substituted transistorized circuits throughout the processing chain. This resulted in an 8 dB SNR increase [Ref01]. Noise limits the amount of gamma correction gain that is practical in the lowlights and thus limits the contrast range of the over-all system
- Stability of the chroma encoding and maintenance of the color subcarrier integrity through the distribution chain (a reason commonly cited for color variations)
- Transmitter differential gain and phase
- Transmitter group delay response
- Stability of consumer receivers
- Lack of coordinated chroma and contrast controls (as a combined “Picture” control) in early consumer receivers
- Lack of full DC restoration in all but the earliest generation consumer receivers
- Changes in receiver phosphors over the years to increase brightness at the expense of colorimetry [Ref02, Ref03, Ref23]
- Early adoption of high color temperature white points in receivers [Ref23, Ref25]
- Adoption of approximate corrective matrices in receivers, which reduced hue errors due to phosphor changes, but introduced saturation and brightness errors in colors other than skin tones; particularly visible as over-bright reds [Ref27, Ref28, Ref37]
- Low contrast capability in early receivers except in darkened rooms due to relatively high-reflectance screens. (The earlier picture tubes could have some internal contrast and purity reduction due to scattered electrons as well [Ref23, Ref26])

- Receiver phase/group delay distortions
- Other distortions peculiar to individual receiver circuit designs

While many factors that affected early color TV cannot be reconstructed today, or can be only partially observed as combined effects in restored video tapes, it turns out that there is enough information available to determine how closely the colorimetry of the early cameras matched the original NTSC phosphor specifications. Furthermore, modern computer programs permit calculating and displaying color results such that they can be viewed on modern displays.

2.1 Order of Presentation for Factors Studied

- Receiver primaries, white point, corrective matrices
 - Affect all colors
 - Based on 3x3 matrix calculations
- Camera gamma correction and noise
- Camera color response
 - Can affect some colored objects more than others depending on interaction of light source, object reflectance spectrum, and camera spectral response
 - Calculated by *integration of product of* illumination spectrum, object spectrum and camera response, plus 3x3 matrix calculations
- Illumination
 - Same calculations as camera color response

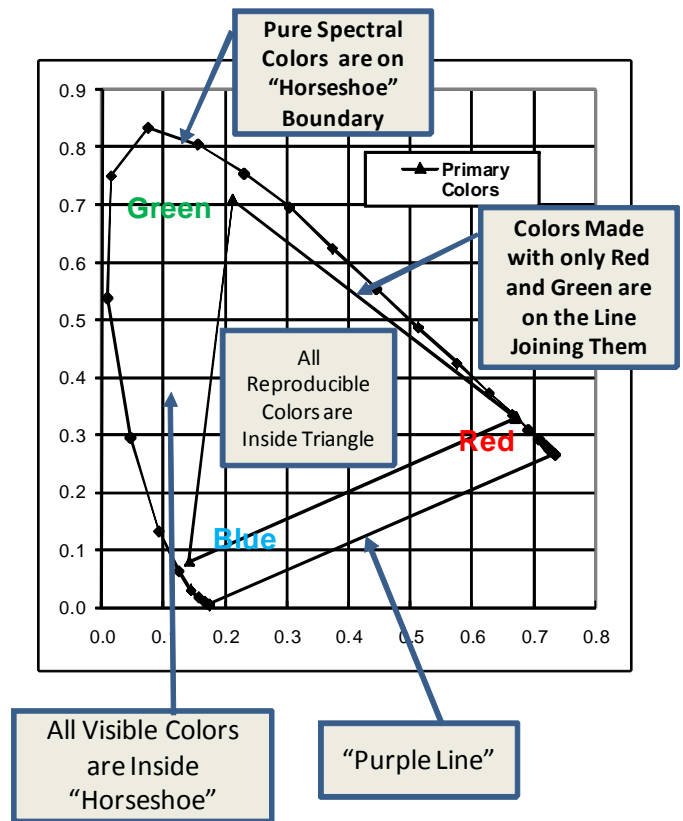


Figure 1 CIE 1931 Chromaticity Chart

The second type of chromaticity chart used is the 1976 uniform chromaticity scale (UCS) chart, which is derived from a projection of the 1931 chart. It has the advantage of being closer to representing equal increments of visibility of color differences in all areas of the chart. The 1931 chart, by comparison, overemphasizes the importance of color differences in the green regions and underemphasizes differences in the blue/violet area.

3 Presentation of Results

Results are presented as spectral graphs, chromaticity charts, and pictures of color charts or natural scenes.

3.1 Chromaticity Charts

Results may be presented on two types of chromaticity charts. The first is the 1931 CIE chromaticity chart:

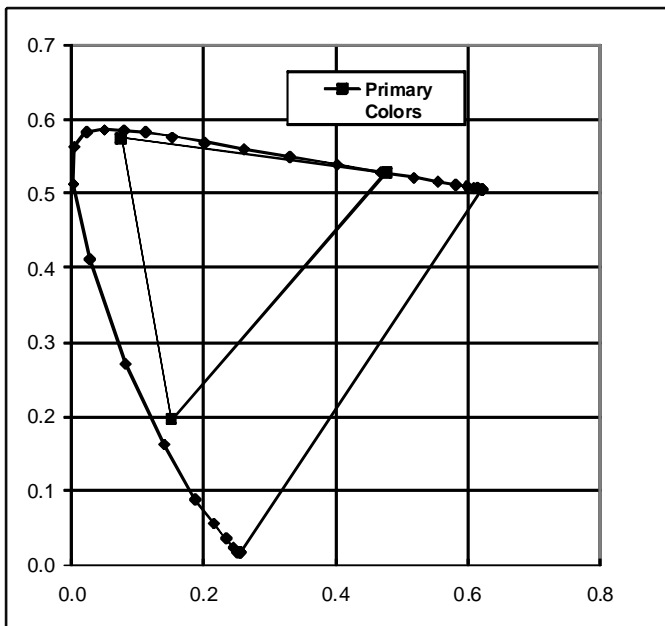


Figure 2 1976 UCS Chart

In both charts, the amount of energy in a light source is ignored, and the two dimensional plot represents only the hue and saturation of a color, and not its brightness. In both charts, the mixture of two colors lies on a line connecting them, and a valid set of primary colors forms a triangle covering some area of the diagram. All colors that are reproducible with a given set of primary colors lie within the triangle joining them. All visible colors lie within a "horseshoe" or "tongue" shaped area.

3.2 Color Chart

SMPTE Standard 303M-2002 defines a color reference pattern for television. This pattern is based on a commercial chart originally designed for use in color photography. It consists of 24 patches of special paints that were formulated to have not only controlled colors but also controlled spectra, some of which mimic natural objects such as human skin or flowers with critical deep-red / near-infrared reflectance. This chart has been studied extensively and data collected by users has been summarized and posted on the internet. Both measured spectra and calculated color coordinates under various lighting conditions are available.



Figure 3 SMPTE 303 M (Macbeth "Colorchecker") chart

3.3 Images

Natural images can be used to illustrate accurately the effects of receiver white point and primary colors. This is done by a 3x3 matrix calculation applied to the color of each pixel. However, because the spectra of objects in an image are unknown, calculations of the effects of camera spectral response are only approximate, and must be based on an assumption that the scene spectra are similar to the color chart spectra. These approximations are nevertheless generally indicative of how a particular camera will affect color reproduction. This paper uses an image of a vegetable market that contains a variety of natural colors.



Figure 4 Vegetable market image

4 Test Colors

Two types of colors may be defined: hypothetical object colors for which only the chromaticity is known; and colors for which the spectrum is known.

4.1 Assorted Colors

These colors have defined chromaticities to cover the primary color triangle more or less uniformly. The spectra are not specified, and therefore these colors are useful only for receiver studies. As shown in Figure 5, the assorted colors (small brown circles) are chosen to be spaced evenly in proportions of the red, green and blue primaries.

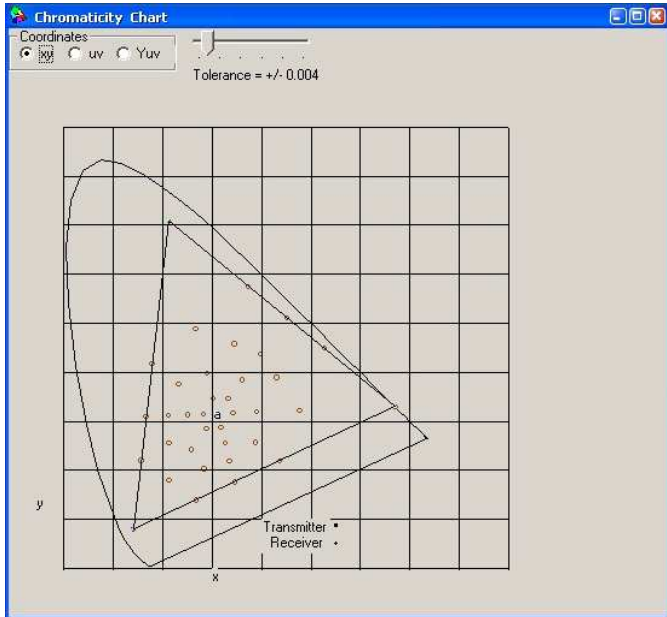


Figure 5 Assorted Colors on CIE 1931 chromaticity chart.

4.2 Chart Colors

These colors are derived from the SMPTE 303M color chart patches, which have known spectra and therefore may be used in exact calculations of the effects of camera spectral response, light source spectrum, etc. These practical colors do not extend to the full saturation possible with the primary colors. (There is one exception: a cyan patch that lies on the edge of the color triangle for some color primary sets.)

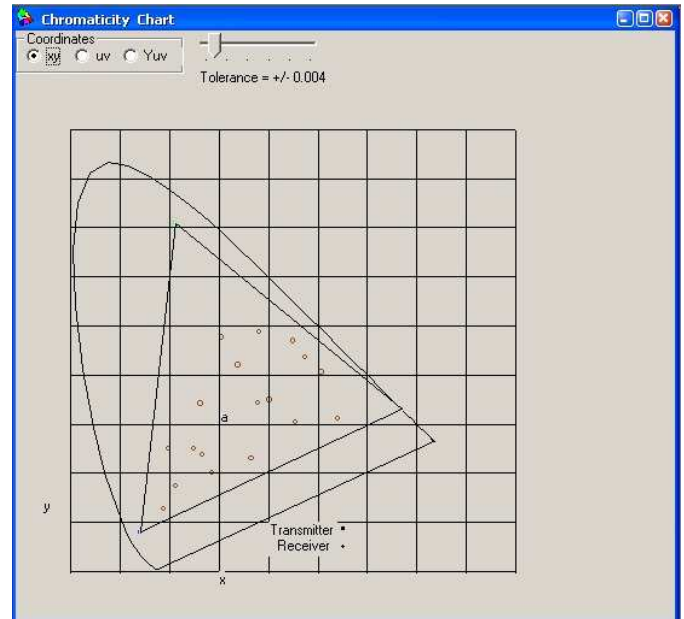


Figure 7 Test chart colors

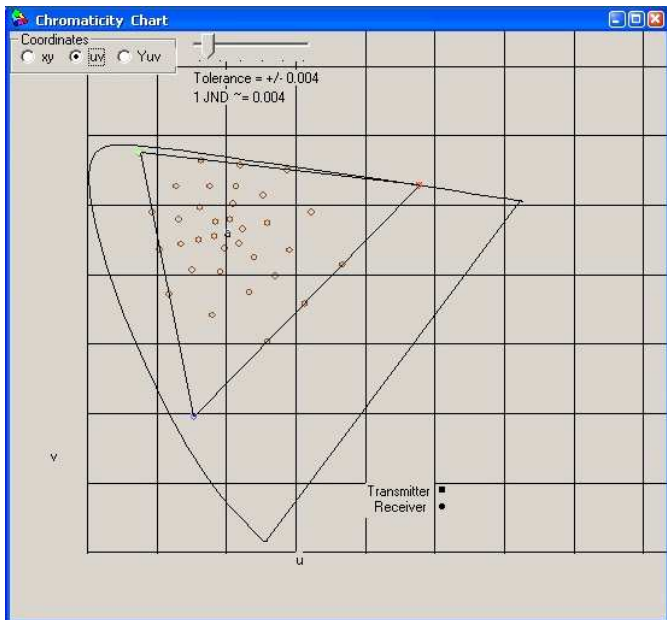


Figure 6 Assorted colors, 1976 UCS chart.

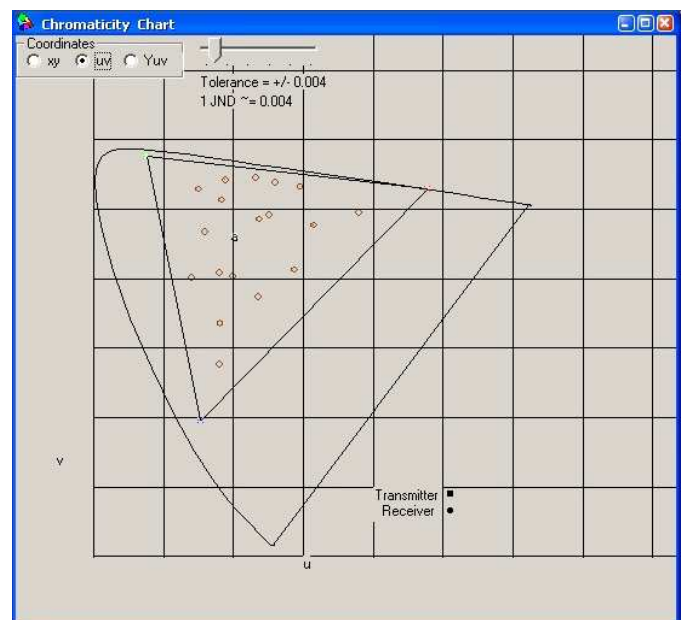


Figure 8 Test chart colors

5 Receiver Effects – Primaries, White Point, and Chroma Demodulator Matrixing

Papers on matrices for approximate color correction in receivers for non-NTSC phosphors and different white points were published by Parker (1966); Neal and DeMarsh (1974), Neal (1975), and Bretl (1979), among others

This section illustrates Parker's results and the tradeoff of color brightness errors for proper flesh tone reproduction

5.1 Results Displayed on UCS Chart and UCS-Brightness Chart

Figure 9 illustrates assorted colors chosen to match the gamut of a standard NTSC receiver.

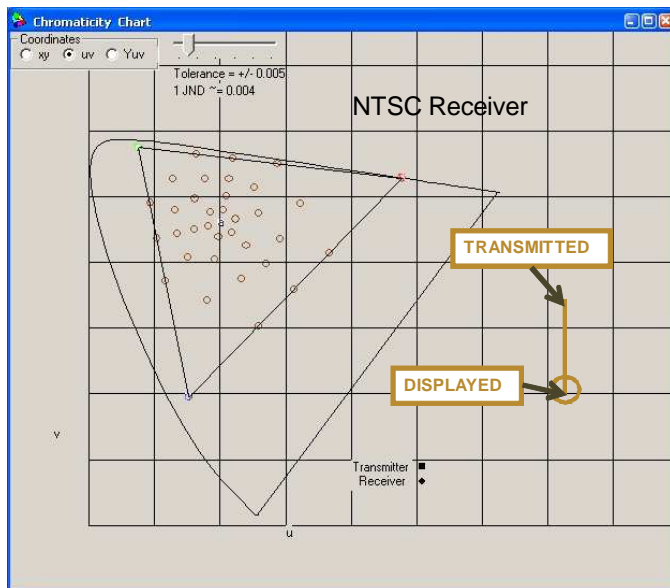


Figure 9 Assorted colors with NTSC camera and display

Figure 10 illustrates the results of change the display phosphors to Parker's primary colors, while maintaining the NTSC white point (Illuminant C). The original and reproduced colors are connected with a brown line, and each reproduced color is at the center of a brown circle.

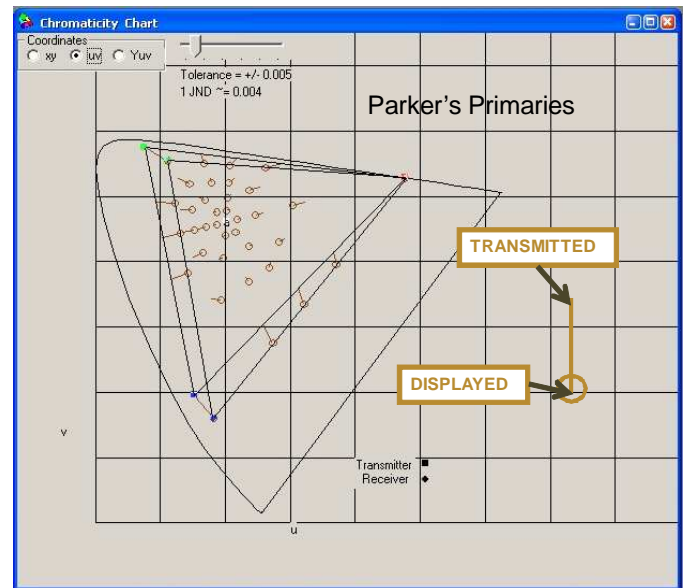


Figure 10 Assorted colors with Parker's primaries

Figure 11 shows the large changes in chromaticity when Parker's primaries are used with a 9300K (cyan-blue) white point. This was a common white point setting for many years in consumer TV receivers.

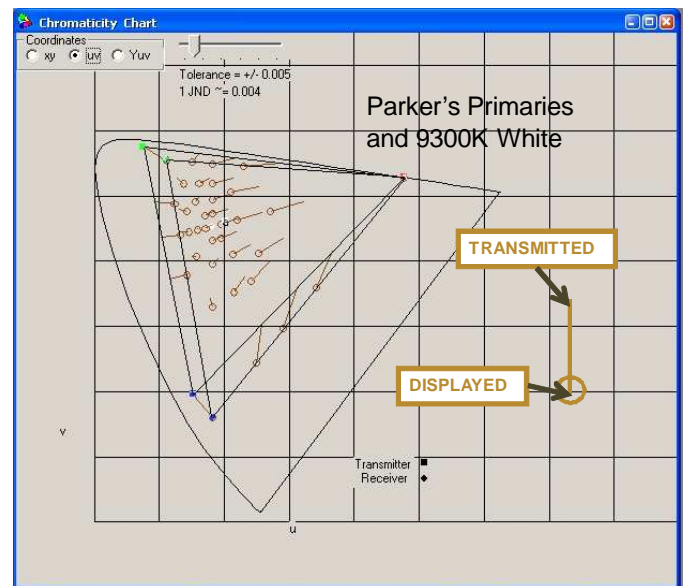


Figure 11 Assorted colors with Parker's primaries and receiver white point 9300 K + 27 MPCD

At this point, we introduce a three-dimensional isometric plot of the colors, in order to show the significant effects on the brightness of colors as well as their chromaticity. In these isometric plots, the vertical axis represents the ratio of the reproduced color's brightness to the original brightness.

In Figure 12, the effects of the primaries and white point appear as a reduction in brightness of reds and magentas, and an increase of brightness of cyans and greens.

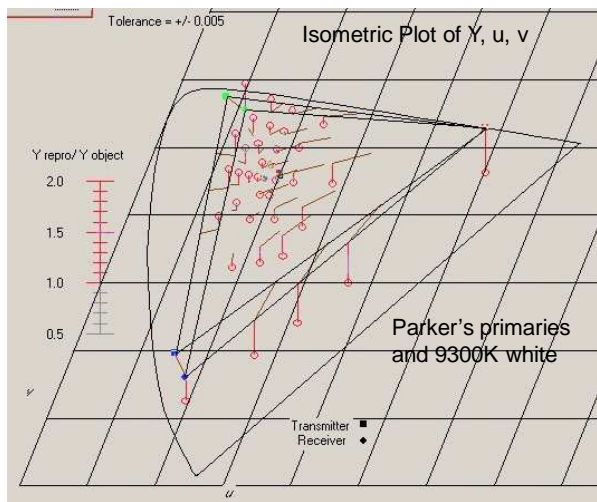


Figure 12 Isometric plot showing brightness distortions

5.2 Simulation of Results for Color Chart and Viewing on Modern Display

The calculations of color distortions are done with respect to a standard NTSC display. However, displays with NTSC primaries are not commonly available. The currently most commonly available display is an sRGB (ITU-R-709, HDTV) display. The results with Parkers' primaries and "9300K + 27 MPCD" white point can be recalculated to drive an sRGB display as long as the output colors are within the sRGB gamut. This is generally the case for the color test chart, except for a very slight error on the cyan color patch, as mentioned above.

The conversion matrix is:

Parker 9300K + 27 MPCD to sRGB

	Rs =	Gs =	Bs =
Rn	0.8632	-0.0157	-0.0156
Gn	-0.1460	1.0726	0.0683
Bn	0.0254	-0.0046	1.1882

In the above matrix, Rn, Gn, and Bn are the values of red, green, and blue in a standard NTSC system, and Rs, Gs, Bs are the values needed to drive a correctly adjusted sRGB monitor to display the actual colors produced on a "Parker" display.

5.3 Parker's Correction Matrix

Parker introduced a method to calculate an electrical matrix for the NTSC chroma subcarrier demodulation that would correct colors for three chromaticities. Only three chromaticities within the primary color triangle can be

corrected, due to the fact that the correction occurs at a point in the system where the signals are non-linear due to gamma correction. (If a linear signal point were available, the correction could be exact for all colors within the primary triangle.) One of the three specified colors must be the new white point. The other two are freely available, and Parker chose a supposed skin tone and grass green color. The matrix converts the NTSC R, G, and B signals to new drive signals Rprime, Gprime, and Bprime to drive the non-standard display.

Parker's correction matrix for 9300K + 27MPCD

	Rprime=	Gprime=	Bprime=
R	1.5468	-0.0187	0.0095
G	-0.1977	0.8960	-0.2231
B	-0.3491	0.1226	1.2135

The effects of primary color changes, white point change, and corrective matrix can be simulated by adjustment layers in a program such as Adobe Photoshop. Figure 13 shows the adjustment layers to achieve this result.

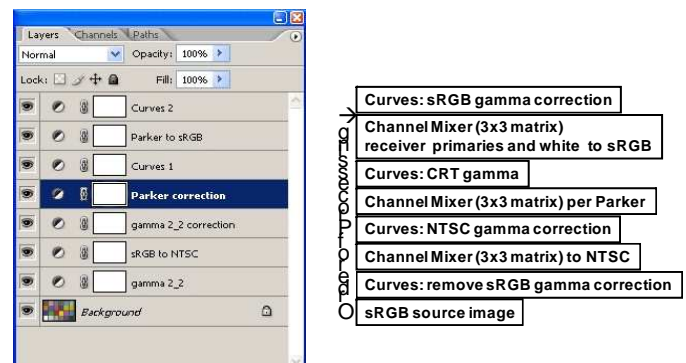


Figure 13 Adjustment layers for simulation in Adobe Photoshop

5.4 Results with Color Test Chart

Figure 14 shows the original (and correctly reproduced) color chart.:

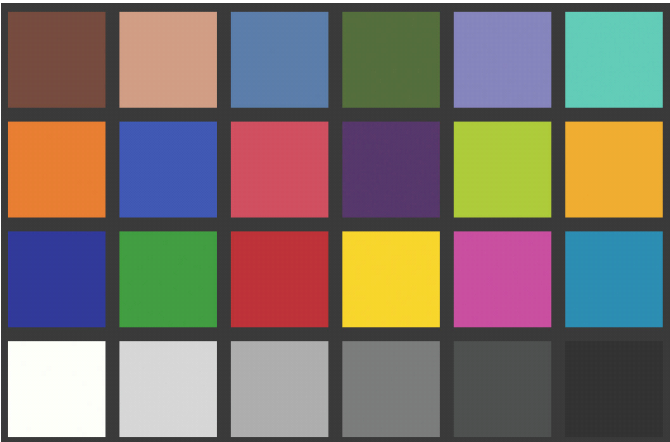


Figure 14 Original test chart colors

Figure 15 shows the changed color reproduction due to using Parker’s primaries with NTSC white point, and no compensating matrix.

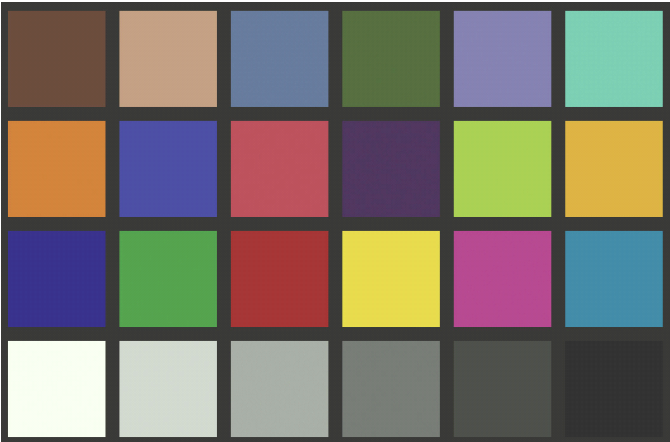


Figure 15 Test chart appearance with Parker's primaries

Figure 16 shows the results with Parker’s primaries and 9300k +27 MPCD white.

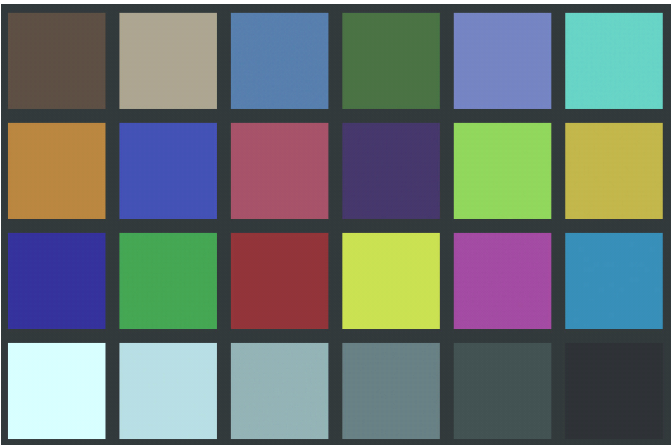


Figure 16 Test chart appearance with Parker's primaries and white point shift

5.5 Parker’s Matrix Effects

Figure 17 shows the results of applying Parker’s correction matrix. Note that the white and gray patches are still cyan, but the skin tones have been corrected to a large extent towards the original colors.



Figure 17 Test chart appearance with Parker's primaries, white shift, and correction matrix

Figure 18 shows the effect of Parker’s matrix applied to his primaries and white point. Note the area of corrected colors within the ellipse.

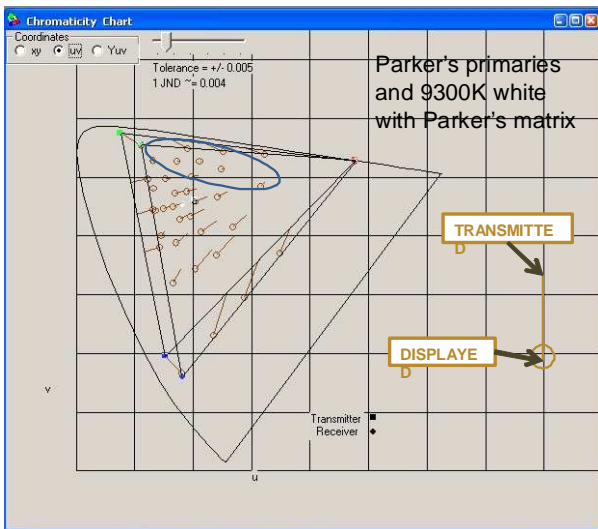


Figure 18 Colors corrected by Parker's matrix

Figure 19 shows the result with assorted colors on the isometric plot. An increase in brightness of the saturated cyan s and especially red is shown.

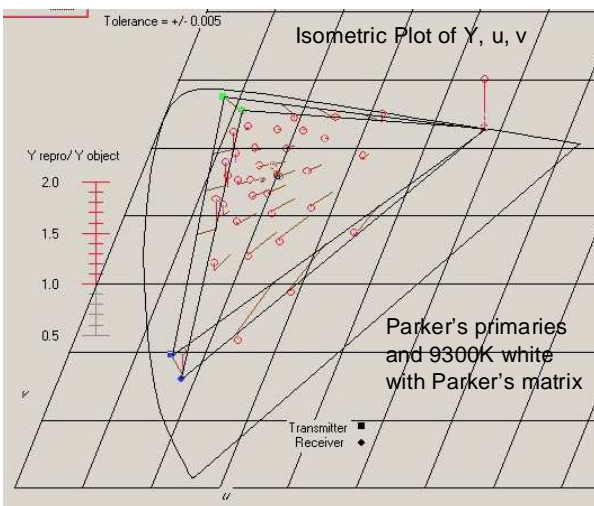


Figure 19 Colors corrected by Parker's matrix

5.6 Higher-Gain Version of Parker's Matrix

Parker designated skin tones that are considerably more saturated than those on the color chart. The result is that the chart skin tones are not fully corrected. On the other hand, a matrix producing stronger saturation of the skin tones results in even more distortion of saturated colors, especially visible in reds.

The effect of Parker's matrix on the color chart is shown In Figure 20. Note that the color chart skin tones (inside the ellipse) are under-saturated.

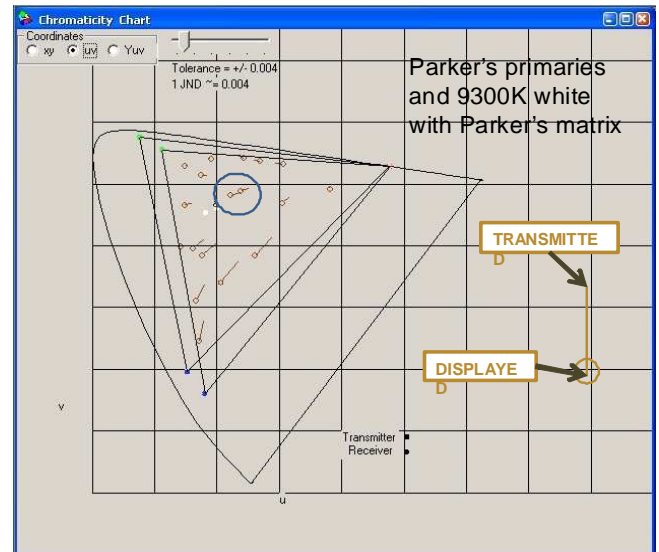


Figure 20 Skin tones under-corrected by Parker's matrix

A matrix with higher chrominance gain (larger cross-terms) can be formed as follows:

Higher-saturation correction matrix for 9300K + 27MPCD

	Rprime=	Gprime=	Bprime=
R	1.7800	-0.0812	0.0476
G	-0.3760	0.9562	-0.3827
B	-0.4036	0.1251	1.4303

Note that the skin tones are now corrected, but saturated reds are strongly overcorrected (Figure 21 and Figure 22).

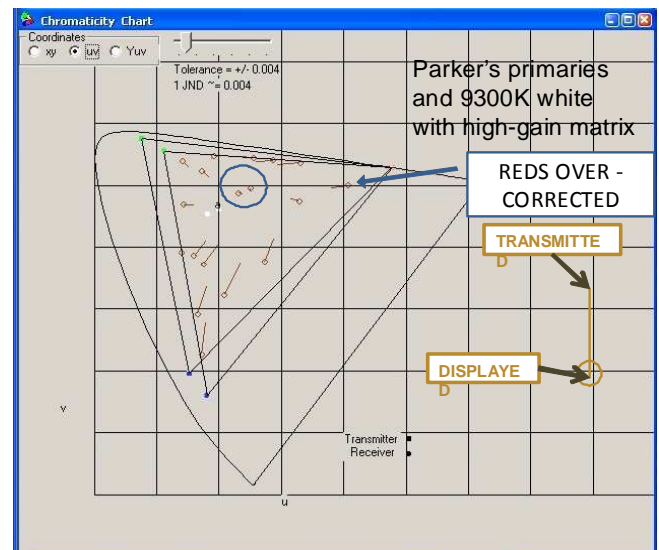


Figure 21 Skin tones corrected and reds overly-bright with high-gain matrix

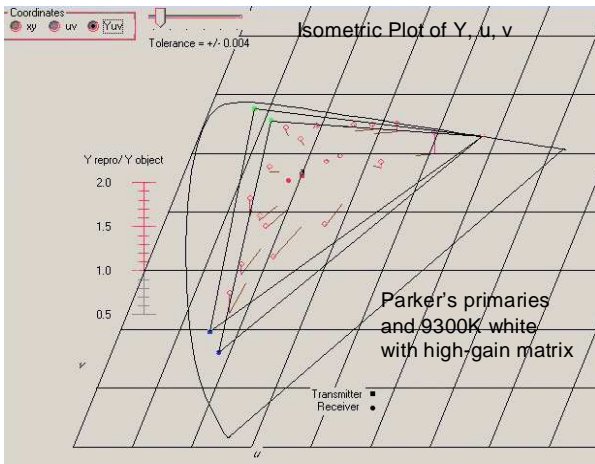


Figure 22 Skin tones corrected and reds overly bright with high-gain matrix



Figure 24 vegetable market with Parker's primaries and white point

Figure 23 shows the result for the color chart with the high-gain matrix, and should be compared to Figure 14 (original) and Figure 17 (Parker's matrix).



Figure 23 test chart appearance with high gain matrix

Figure 24, Figure 25, and Figure 26 show the results on the "vegetable market" image. These images should be compared to the original in Figure 4. Note that while the high saturation matrix corrects the test chart skin tones, it is noticeably oversaturated for more saturated colors, and exaggerates the variations in skin tones due to the mixed natural and incandescent lighting in this image.



Figure 25 Parker's primaries and white point, with Parker's correction matrix.



Figure 26 Parker's primaries and white point, with high-saturation matrix

5.7 Net Results of Receiver White Point, Primary Colors, and Corrective Matrix

Matrixing in the receiver to compensate the shift in the green primary color towards yellow resulted in some brightening of reds. Attempts to adjust for a 9300 K white point resulted in even stronger distortions of saturated reds. Furthermore, an approximation to the higher gain matrix was available to the viewer in the form of the "color" (chroma gain) control, and depending on the viewer's preference, the equivalent of a

high gain matrix could be introduced at will. As will be seen in following sections, the resulting receiver color errors would be significantly larger than those introduced by the studio camera designs.

6 Image Orthicon Color Cameras

6.1 Pre-Production, 1949-1953, Plate Optics

The early cameras used dichroic mirrors built on flat glass plates, and separate Corning and Wratten trimming filters to adjust the color response in the red, green and blue (RGB) channels [Ref04, Ref05, Ref06].

6.2 Later Production, Prism Optics

Prism optics were developed for the TK-41 series of cameras, and were often retrofitted to older cameras. The prism assembly had permanently-mounted trimming filters. It is believed that these may have been based on interference filters rather than the Wratten (gelatin) and Corning (glass) absorptive filters used with the older plate optics, and therefore are less likely to have faded over time.

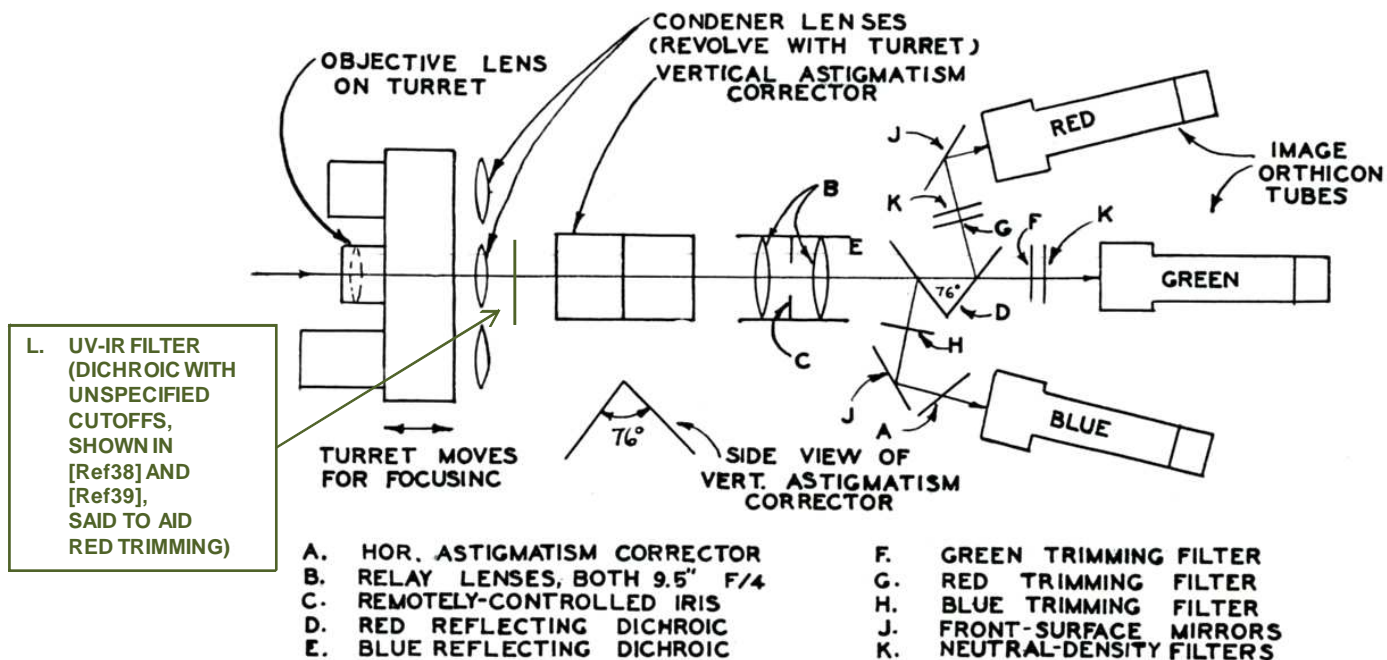


Fig. 9 – Sketch of the optical system used in an RCA three-tube color television camera.

Figure 27 Plate Optics (from [Ref04])

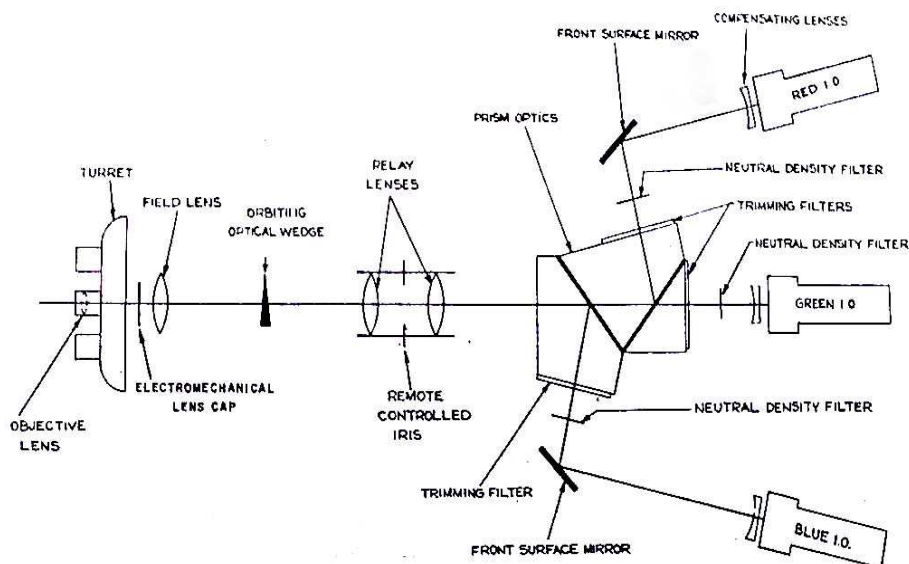


Figure 28 Prism optics [Ref05]

7 Gamma Correction and Noise

7.1 Gamma Correction Basics

Basically, gamma (γ) is the exponent in the function that describes the beam current (hence brightness) in a cathode ray tube (CRT) as a result of the video voltage input: $I = V^\gamma$

Gamma correction is the inverse: $V = I^{(1/\gamma)}$, and is applied in the camera to each primary channel (R, G, and B).

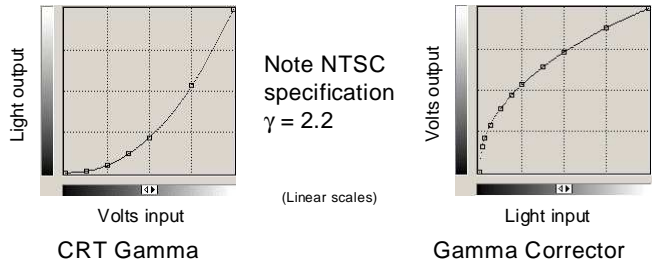


Figure 29 CRT Gamma and Gamma Correction

7.2 Gamma Correction Problems

The ideal gamma correction has infinite gain (slope of the correction curve) near black. This is impossible in real circuits. Even very high gain is impractical because of the resulting amplification of imaging device noise in the lowlights.

However, limiting the gain sets an implicit limit on contrast ratio of the system, since video below a certain level will be attenuated by the CRT gamma. Even with limited gain, pickup device noise is amplified in the lowlights. This noise obscures the shadow detail and is partially rectified, raising the black level

7.3 TK-41 Gamma Correction

The image orthicon was a much noisier device than current devices. The original type 5820 had a specified signal to noise ratio (SNR) of 35:1 (31 dB). (The SNR is specified as the ratio of black-to-white signal range divided by rms noise.) At 34:1 SNR, the noise is definitely visible in the picture, and gamma correction gain near black needs to be limited to prevent the noise from being objectionable. (Modern pickup devices may have a SNR of 60 dB or more {1000:1}.)

The TK-41 camera gamma correction circuit was designed to correct for a gamma of 1.4 instead of 2.2. It was accomplished using a piecewise-linear amplifier load with two breakpoints. In addition, there was an initial attempt to use

highlight compression inherent in the image orthicon under certain operating conditions.

The following figures show the TK-41 circuit, the aim transfer function, and the transfer curve obtained. Incremental gains (slopes) are 1.6, 0.8, and 0.6.

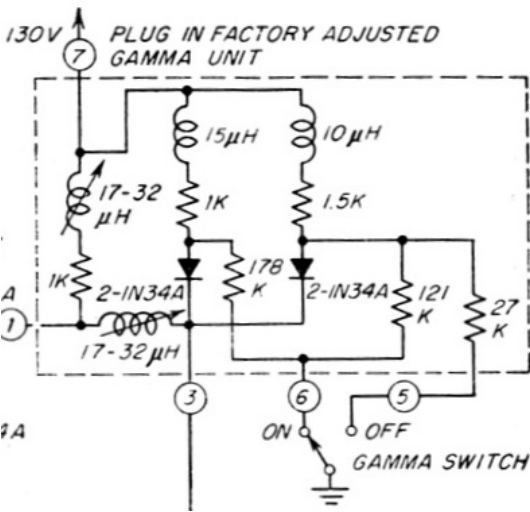


Figure 30 TK-41 gamma correction circuit

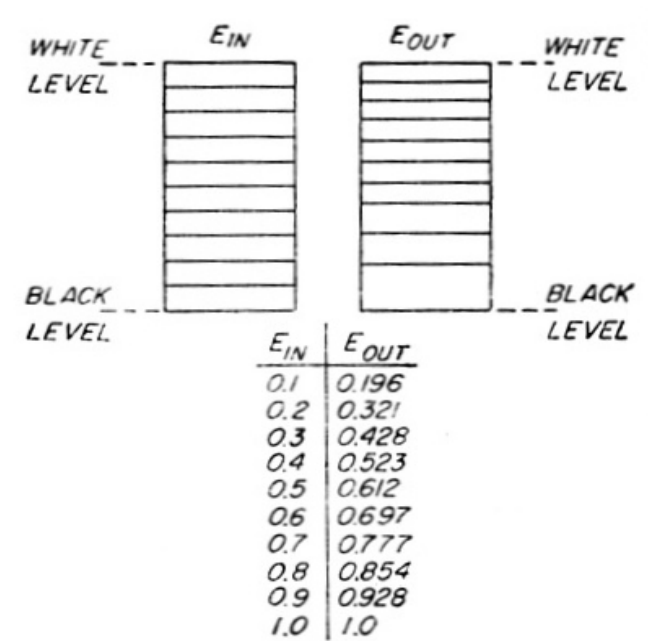


Figure 31 TK-41 gamma corrector aim - 0.707 power law

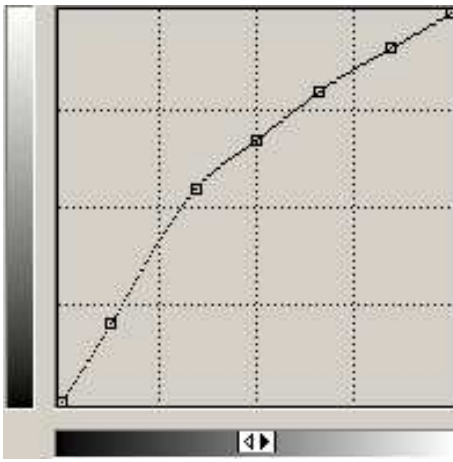


Figure 32 TK-41 gamma corrector transfer function

Figure 33 shows the highlight compression obtainable with use of 2 volts on the target. This operating condition was perilously close to producing dark halos around bright objects due to electron re-distribution. In the case of a bright colored object, the halo would be a complementary color. For example, a bright red dress might produce a cyan halo extending onto the performer's face. This curve is also a poor fit to the needed gamma correction, even as an adjunct to the non-linear gamma correction circuit. It was therefore abandoned in favor of a 4-volt target setting to keep highlights from showing halos. Scenes "properly exposed" would then have no highlight compression.

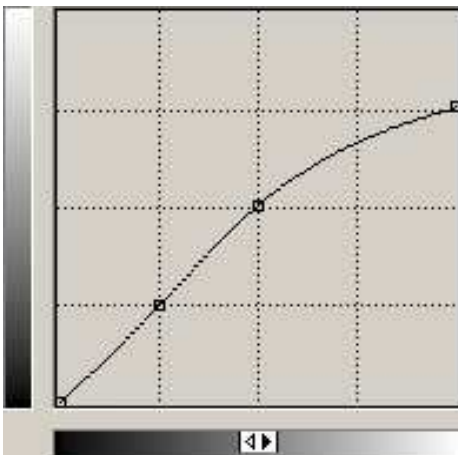


Figure 33 Image orthicon highlight compression with 2 volts target voltage

The combination of image orthicon highlight compression and the non-linear amplifier gives a maximum slope of $1.6/0.75 = 2.13$

This compensates for the CRT at a level where its slope is $1/(2.13) = 0.469$, which implies the video signal is 0.276 and the light output is $(0.276)^{2.2} = 0.0587$

The system contrast range (for output roughly proportional to input) then is:

$$1 / 0.0587 = 17:1$$

Note that modern systems (with much lower-noise cameras) typically specify a gamma correction curve that gives a system contrast ratio of several hundred. For example, the sRGB specified maximum slope is 12.92. This implies that the contrast ratio is 463:1

The two left graphs in Figure 34 show that the TK-41 gamma correction circuit results in large errors in the mid tones and lowlights of the picture. However, an increase in the black level prior to the gamma corrector (an adjustment readily available to the video engineer) results in much improved midtone reproduction, at the cost of some fogginess in the lowlights. The author surmises that this was the actual operating condition generally used.

Figure 34 shows the transfer functions for four combinations of operating conditions. The left column of graphs shows the stage-by stage results with no black level lift, while the right column includes a 10% black level lift. The top row includes compression of highlights due to the use of a 2-volt target voltage, while the bottom row shows linear highlights due to use of a 4-volt target voltage. The bottom row is therefore the normal set up in a color camera, and the bottom right graph is the surmised condition with black level lift.

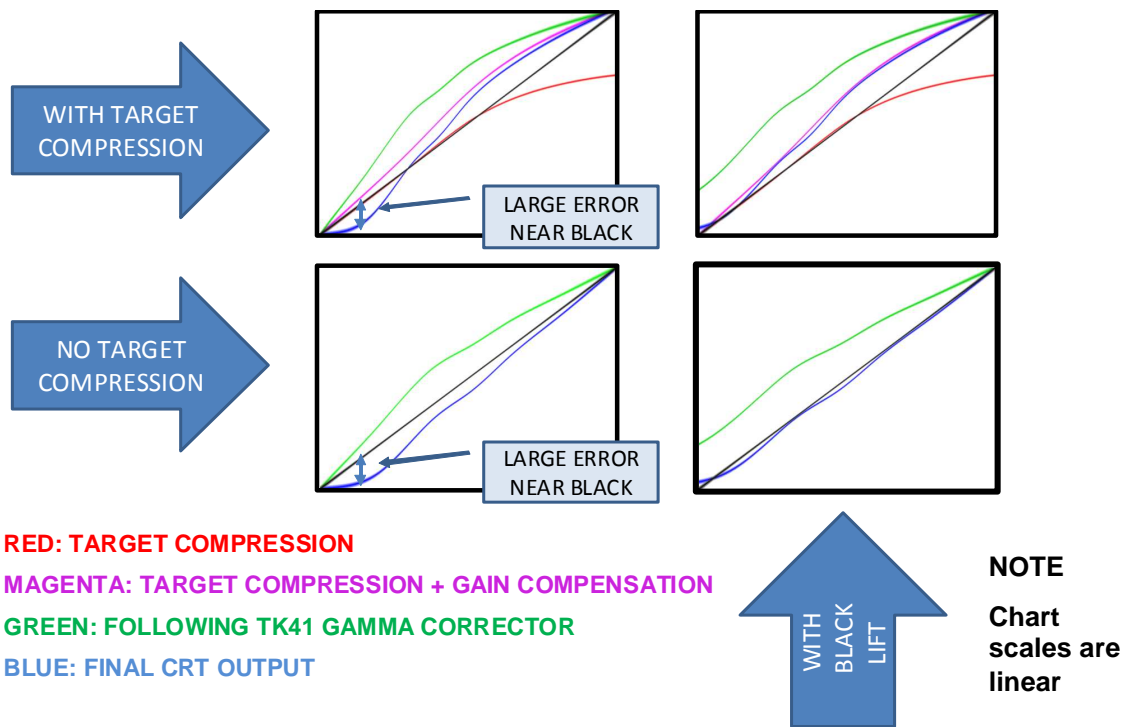


Figure 34 Gamma correction with different TK-41 adjustments

Figure 35 through Figure 44 show the results with various stages of the gamma correction in operation, and also with and without noise present. Figure 43 and Figure 44 show the effects of noise in conjunction with a high gain gamma corrector, to show the undesirable amplification of noise in the lowlights. Noise is illustrated at two levels: 31 dB is the SNR specified for the type 5820 image orthicon, which was the “workhorse” for monochrome cameras. 36 dB is the SNR specified for the type 8474 and similar image orthicons, which had a smaller target-mesh spacing and therefore an extended highlight range below the “Knee” (the level where highlight compression and electron redistribution begins).



Figure 36 Gamma correction off, SNR = 31 dB



Figure 35 Gamma corrector turned off



Figure 37 Gamma correction off, 31 dB SNR, with highlight compression (target voltage = 2 V)



Figure 40 Target voltage 2 V, black level raised 10%, gamma corrector ON, SNR = 31 dB



Figure 38 conditions as for previous figure, with gain increased to restore peak white level.



Figure 41 Linear highlights (target voltage 4 V), black level raised 10%, gamma corrector ON, SNR = 31 dB



Figure 39 Target voltage 2 V, gamma corrector ON, SNR = 31 dB



Figure 42 Improved image orthicon (type 8474) - Linear highlights (target voltage 4 V), black level raised 10%, gamma corrector ON, SNR = 36 dB



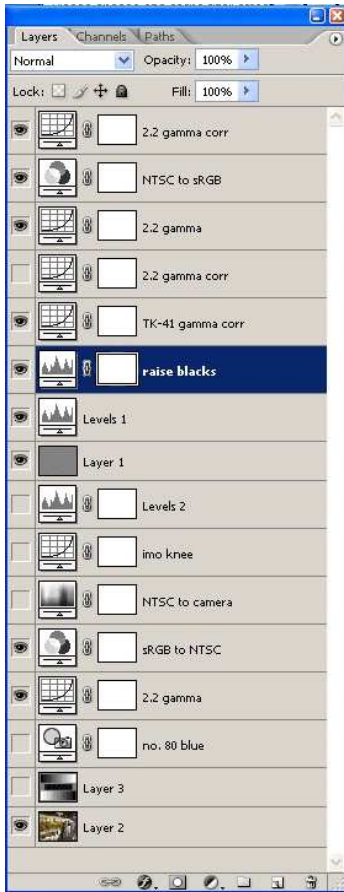
Figure 44 SNR = 36 dB, high gain gamma corrector (maximum slope = 9.75) (contrast ratio = 276:1)



Figure 43 SNR = 31 dB, high gain gamma corrector (maximum slope = 9.75) (contrast ratio = 276:1)

7.4 Simulation Technique

The images illustrating gamma correction and noise were generated in Adobe Photoshop using the layers shown in Figure 45.



- ← 1/(2.2) gamma correction curve for sRGB output
- ← NTSC to sRGB matrix (channel mixer)
- ← 2.2 power curve of NTSC CRT
- ← 1/(2.2) gamma correction curve may be substituted for TK-41 curve
- ← TK-41 gamma correction curve
- ← Black lift prior to TK-41 gamma correction curve
- ← Restore image contrast lost due to noise layer opacity
- ← 127 mid-gray with 15% Gaussian noise – opacity 10% or 16% to vary noise
- ← Peak-to-Peak gain restoration for target compression
- ← Image orthicon target compression curve
- ← Approximate NTSC to Camera (Hue, Saturation, Lightness adjustments)
- ← sRGB to NTSC matrix (channel mixer)
- ← 2.2 power curve to linearize sRGB input
- ← Color balance filter if required
- ← Substitute grayscale image for histograms
- ← Base image (sRGB)

Figure 45 Processing layers for simulation of gamma correction and image orthicon noise

7.5 Histograms

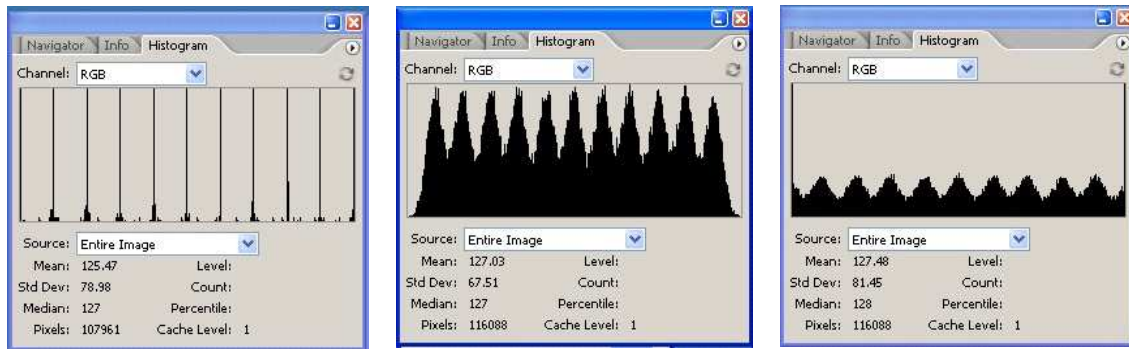
Histograms of a gray-scale pattern help to understand both how the simulation works and the effects of the camera circuits.

Figure 46 shows the operation of the noise addition in Photoshop. A layer consisting of a mid gray level (127) with added Gaussian noise is superposed on the image with a certain percent opacity. The “blend mode” is “normal.” The left histogram of Figure 46 is that of the original gray scale image. The center histogram shows the result of adding the noise gray layer. While the noise is added linearly as desired, there is also some addition of gray, so that the range from

black to white is reduced. A “levels” adjustment layer above the noisy gray layer restores the contrast of the original image. This increase in contrast also applies to the noise, so that the added noise level has to be pre-calculated to become the desired level in the final image.

Figure 47 shows the effects of the gamma correction without and with black level lift, but without noise so that the effects on the gray steps are clearly visible.

Figure 48 shows the histograms with noise present. For these charts, the SNR of the improved image orthicon is used to make the levels more easily distinguishable.



11-Step Grayscale → With 15% Noise Layer, 16% Opacity → With Level Adjustments
 $SNR = 35:1$
 $= 31 \text{ dB}$

Figure 46 Addition of noise with noise layer and levels adjustment layer

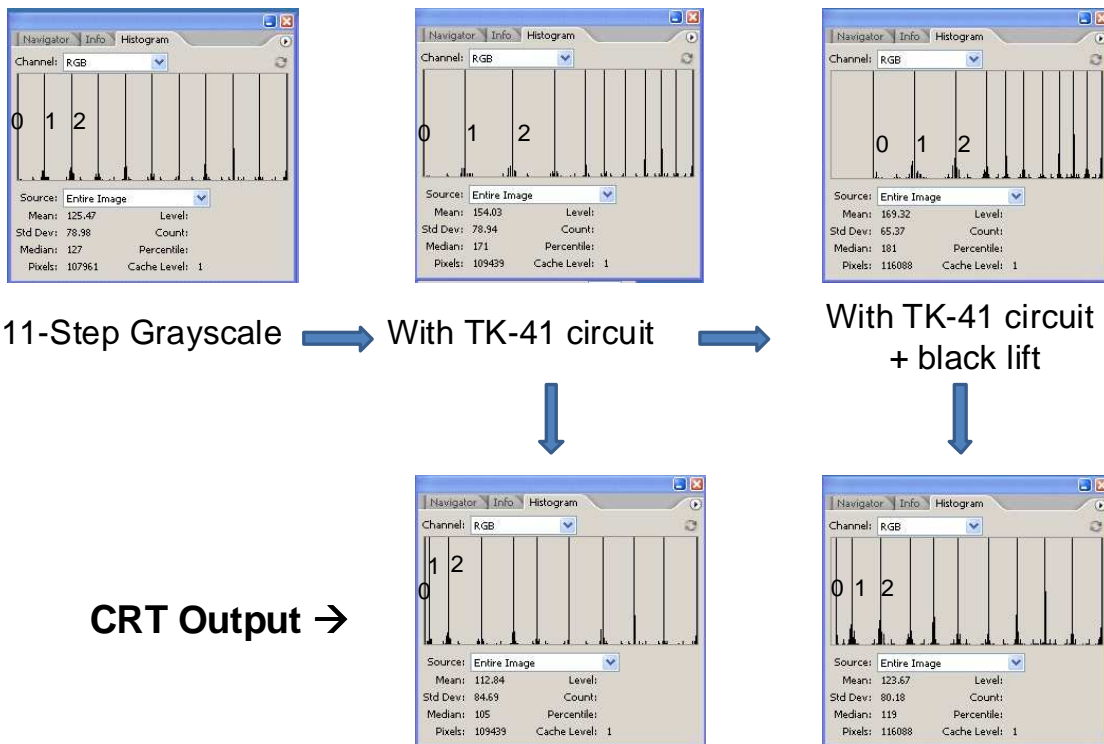


Figure 47 Gray levels with TK-41 circuit and black level lift

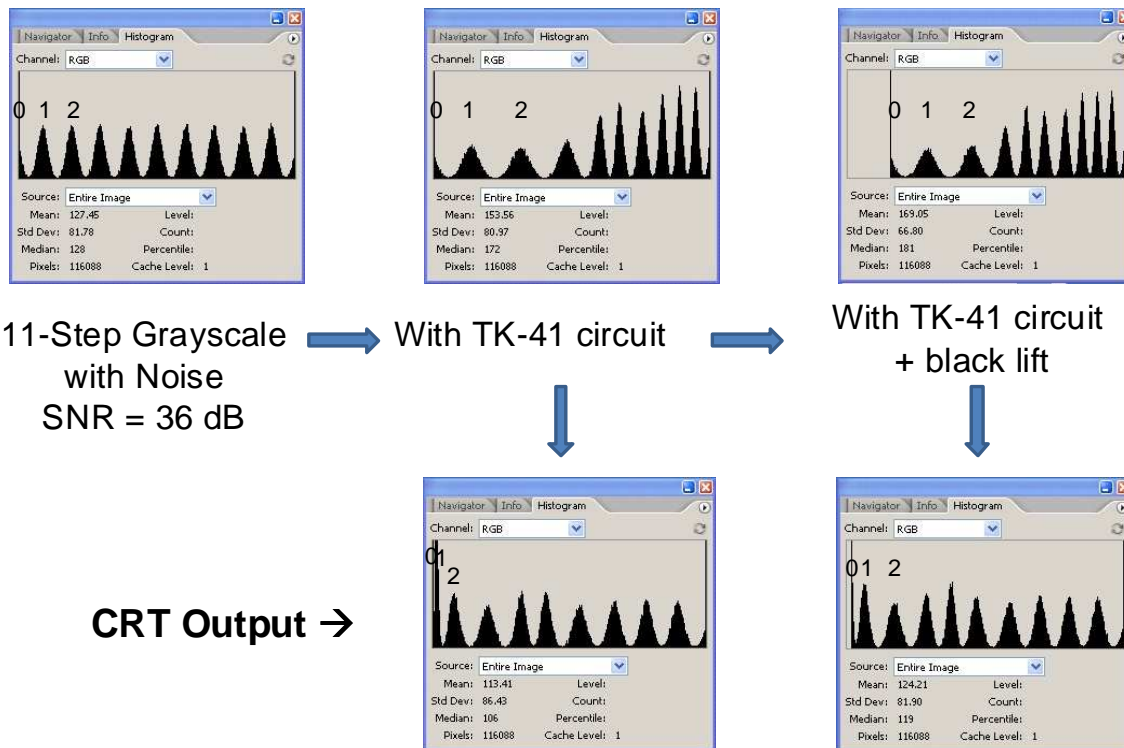


Figure 48 Gray-scale histograms with noise

8 Analysis of Color Reproduction

8.1 Calculations for Test Objects of Known Spectra

8.1.1 Assumptions

8.1.1.1 Illumination

The assumption was made that the scene was illuminated by Illuminant C. Although modern systems assume D65, the choice was made to use the same artificial daylight specification for input and output, even though the results would be viewed on a modern monitor operating at D65. That is to say, a matrix calculation could have been applied to make a modern monitor produce Illuminant C when viewing the output files, but this was not done. Spectral values for the illuminants are found in [Ref07] and [Ref08].

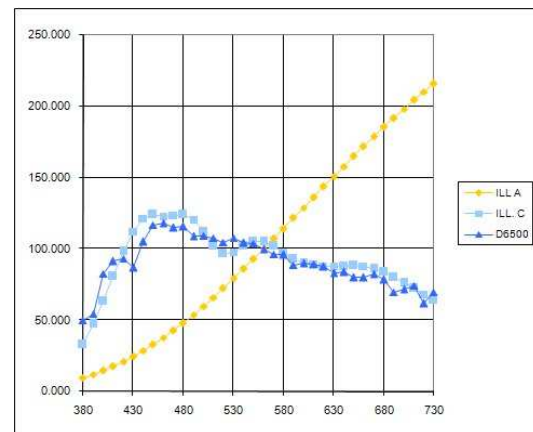


Figure 49 Standard Illuminants

Calculations were also made assuming illuminant A (low color temperature incandescent light) at the scene. This was done to study the result of the effective change in taking characteristics (spectral responses) due to the slope of the Illuminant A spectrum. Figure 49 shows the spectra of the three illuminants. (Note: unless otherwise stated, all figures showing spectral curves have wavelength in nm on the horizontal axis and arbitrary units on the vertical axis.)

There are basically two ways to adjust a three-channel color camera for white balance under different illuminants. One way is to insert a color filter that adjusts the spectrum of the illumination to match daylight. This follows the philosophy

that the system is expected to reproduce colors as they would appear under daylight, and is the approach taken here to study the base colorimetry of the cameras. The second method is to simply adjust the gain of each of the three channels to achieve white balance. This is what was actually done in the early cameras (by means of different neutral density filters in each color channel), and it results in some shift of the “cross-over points” (wavelengths of equal response) of the three color channels towards red under tungsten light, compared to the daylight case. It is possible that a given camera spectral response will, when combined with Illuminant A, result in correct reproduction as though Illuminant C had been used. In this case, the reproduction under daylight will be less accurate unless a color correcting filter is used.

8.1.1.2 Displays and Primaries

A majority of the error calculations were done for NTSC phosphors, as they represented the target display by 1953. Some calculations were also done for the early trinoscope display and a hypothetical reduced gamut display presented briefly in [Ref04]. From [Ref04], it appears that the camera design may have been aimed at the trinoscope display, which had a slightly different green primary, even less yellow than the NTSC green, giving a somewhat larger gamut in the cyan area. The trinoscope also had a significantly more violet blue primary.

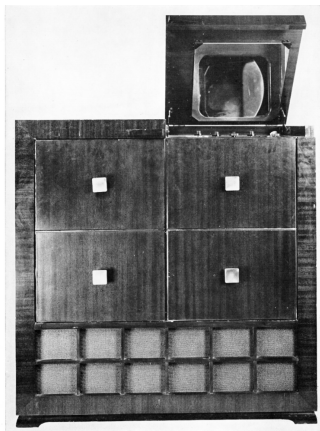


Fig. 1—Trinoscope Receiver Model No. 1

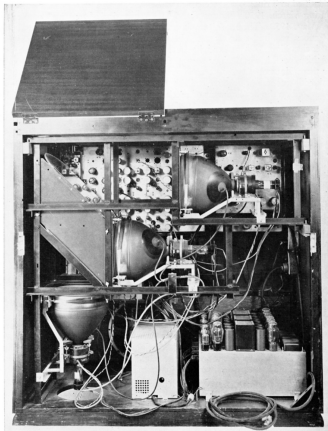


Fig. 2—Trinoscope Receiver Model No. 1

Figure 50 RCA Trinoscope #1 [Ref04]



Fig. 3—Trinoscope Receiver Model No. 2

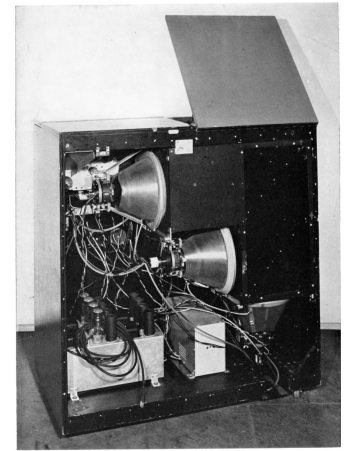


Fig. 4—Trinoscope Receiver Model No. 2

Figure 51 RCA Trinoscope #2 [Ref04]



Figure 52 Six-inch Trinoscope shown by Mitsubishi at the New York World's Fair 1964-1965 (left and upper right) and screen photo of operating unit from the collection of Erich Loepke (member trinoscope on audiokarma.org) (2007)

Tables of color errors for certain test objects when picked up by various cameras and viewed on the trinoscope are presented in [Ref04]. Unfortunately, as seems to have been a frustrating common practice over the years, the spectra of the test objects was not published, and therefore the results cannot be duplicated.

The earliest camera for which data was published in [Ref04] has a green response that is not proper for any of the phosphor sets that are also published there, although it was used in a demonstration in October 1949. No explanation is

given for this discrepancy, but calculated color errors are presented, leading one to believe that it is presented in [Ref04] for completeness and/or as an attempt to explain visible errors in the demonstration. The resulting errors are illustrated below.

The displays considered in this paper are:

- Parker’s all-sulfide phosphors (see the relevant section above)
- Trinoscope – earliest display, high-purity primaries
- Reduced gamut – mentioned in [Ref04], but abandoned
- sRGB – used only for conversion of illustrations to modern displays

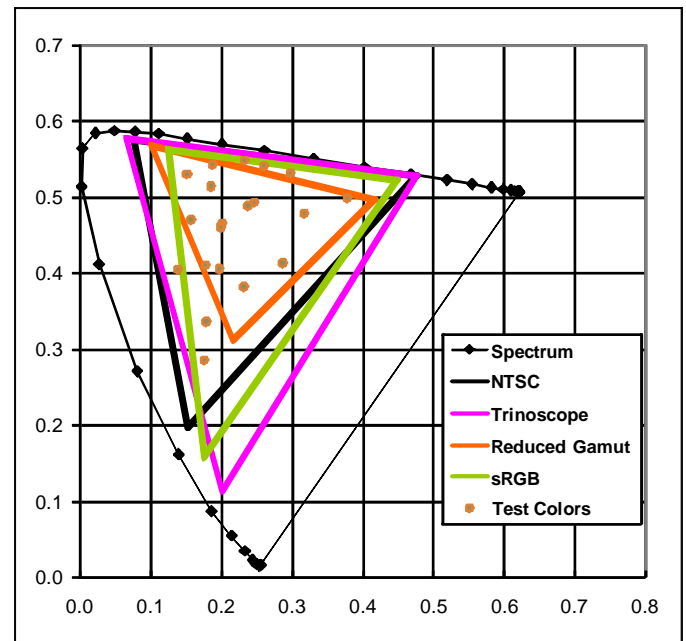


Figure 54 Primary color sets (1976 UCS chart)

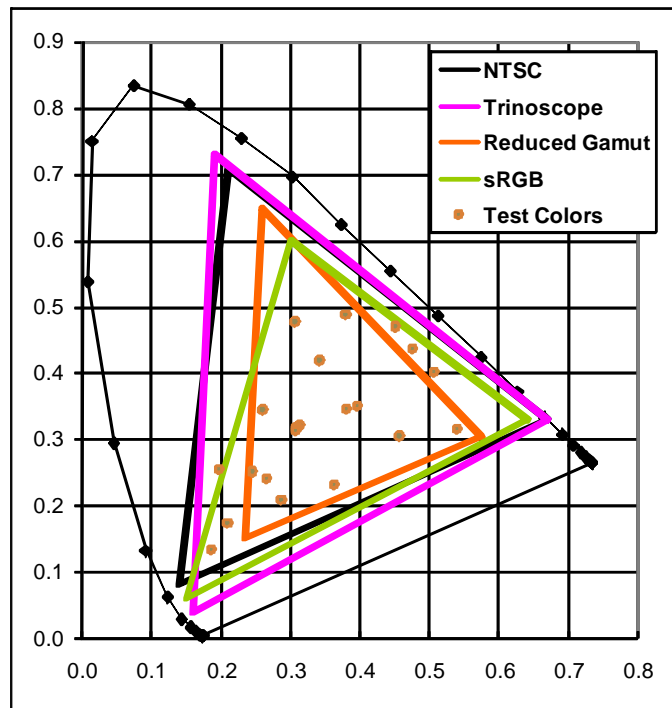


Figure 53 Primary color sets (1931 CIE chart)

No error calculations were done for the case of a vintage camera used with modern display phosphors. Correction matrices for this case have been the subject of many papers (see [Ref09] for examples), and are illustrated for the case of an ideal NTSC camera in the section on Parker’s matrix above. However, colors in all resulting images in this paper were adjusted in a final series of steps to make them reproduce correctly when viewed on a modern sRGB display [Ref10, Ref11, Ref24].

8.1.1.3 Calculation of ideal taking characteristics

“Taking characteristics” or “color matching functions” are the camera spectral responses needed to specify the amount of each primary color to reproduce the appearance of pure spectral colors. The fictional CIE primary colors lie outside the “horseshoe” curve that contains all real visible colors, and therefore have all-positive color matching functions.

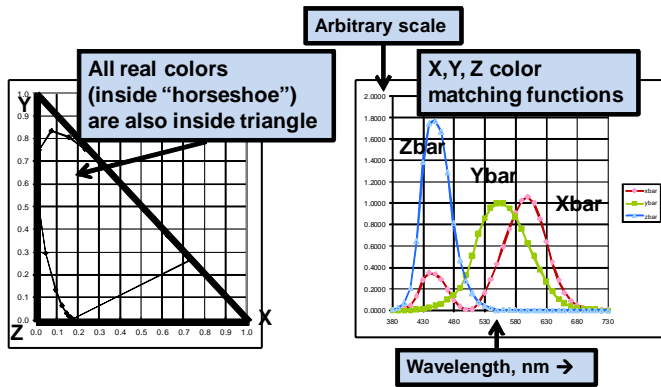


Figure 55 X, Y, Z color matching functions

Proper taking characteristics for real primary colors are always a linear combination (via a 3x3 matrix) of the CIE X, Y, Z matching functions. However, since real primaries never encompass the whole area of visible colors, they will require negative responses to some wavelengths in order to reproduce correctly the colors that are within their gamut.

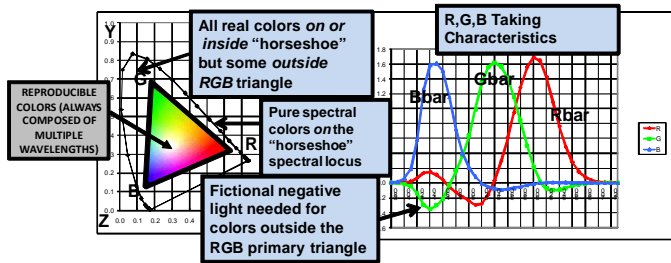


Figure 56 Taking characteristics for a set of real primaries

Ideal taking characteristics for various displays are shown in the following figures.

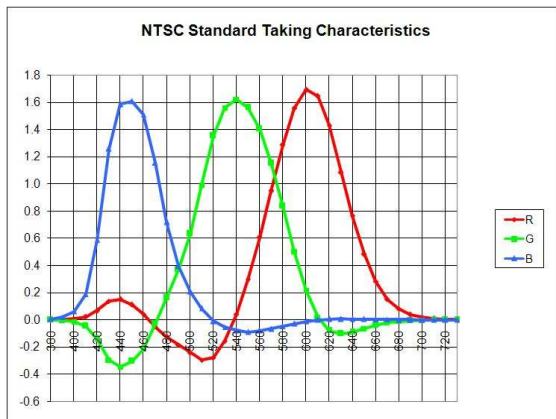


Figure 57. Ideal NTSC taking characteristics

Figure 57 shows the ideal taking characteristics for the NTSC primaries. It should be noted that the negative lobes are not large in amplitude or area compared to the positive lobes. This allows a compromise in a practical camera. Instead of

providing these negative lobes, the correct response to object spectra may be approximated by using narrowed versions of the positive lobes. This is the method used traditionally in most color photographic films, and also used in the early television cameras. In television cameras, this technique was desirable since a matrix impacts the signal-to-noise ratio of the camera. Some later photographic films included a layer or layers sensitive to the negative-lobe regions and producing an opposing action to the associated primary color layer.

The exact negative lobes needed could be obtained by a camera with nine different positive spectral responses, or by a camera with three all-positive spectral responses equal to the CIE X, Y, Z curves, followed by a matrix. These methods have not been used due to the difficulty of providing extra sensors and also the optical inefficiency of splitting the incoming light into smaller portions of the spectrum.

When less noisy pickup devices became available, linear matrixing of three sensors to obtain approximations to the correct positive and negative lobes became the common practice.

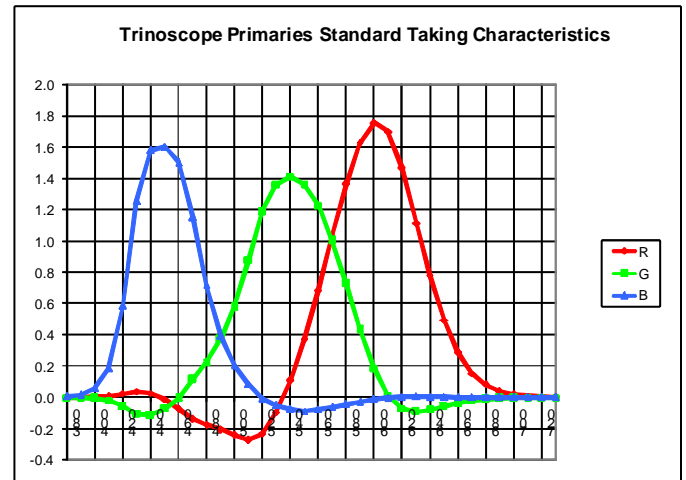


Figure 58 Taking characteristics for trinoscope

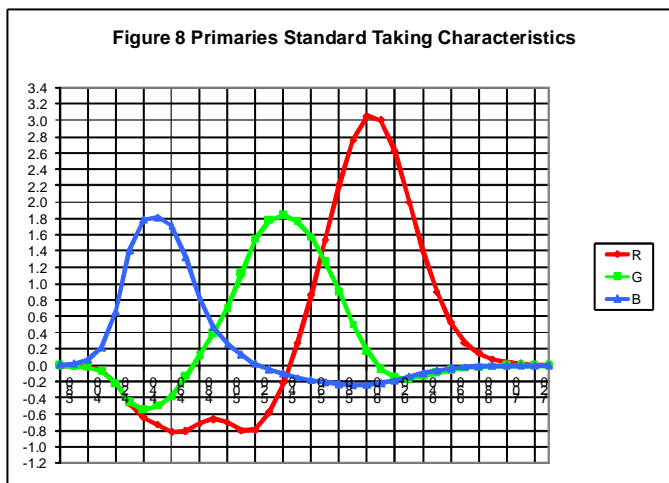


Figure 59 Taking characteristics for reduced-gamut primaries specified in figure 8 of [Ref04]

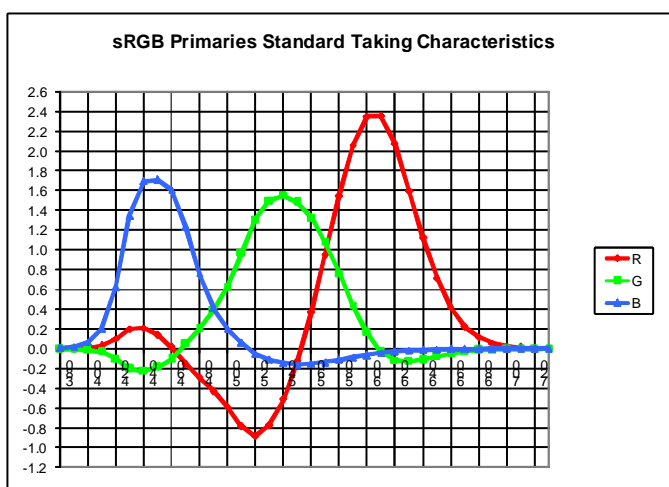


Figure 60 Taking characteristics for sRGB primaries

8.1.2 Ideal Reproduction for Comparison

The ideal reproduction was calculated by the same method as the camera response, except that human eye color matching functions were substituted for the camera RGB response curves, and the RGB values for an sRGB display were calculated. Color matching functions are found in [Ref07] and [Ref08].

8.1.3 Possible Improvements to Early Cameras via Linear Matrixing

Although the possibility of improving color rendition by linear matrixing was known at the time, it was rejected on the grounds of complexity and decrease in the SNR of the video. In later camera development, it was realized that the color separation optics could be designed for increased transmission by eliminating highly absorptive trimming filters, and the resulting color errors largely corrected with a matrix,

resulting in good SNR and good color. In addition, the greatly improved sensitivity of later pickup devices made this a much less severe tradeoff [Ref12, Ref13]. Additional work on camera color analysis can be found in various SMPTE Journal papers, some of which are collected in [Ref09].

The matrix design calculations generally proceed by a least squares optimization of the reproduction of a set of test objects with known spectra [Ref14]. The reproduced colors (actually, their RGB levels) may be obtained either by practical measurement with an actual camera, or by calculation if the spectral response of the camera is known. The resulting matrix is influenced by the choice of test objects, of course, and in general cannot be perfect unless the camera RGB responses are linear combinations of the color response functions of the human eye. For a general discussion of this topic, see [Ref07].

As part of this exercise, a corrective matrix was calculated for each camera to assess how much improvement might have been made if SNR were not a problem.

8.1.4 Input Data

Camera spectral responses were obtained two ways:

1. From recorded over-all RGB spectral response curves
2. From curves of individual system components either published or measured

Curves of the over-all RGB responses from [Ref04] and [Ref15] in graphic form were transposed manually by reading the values from printed copies.

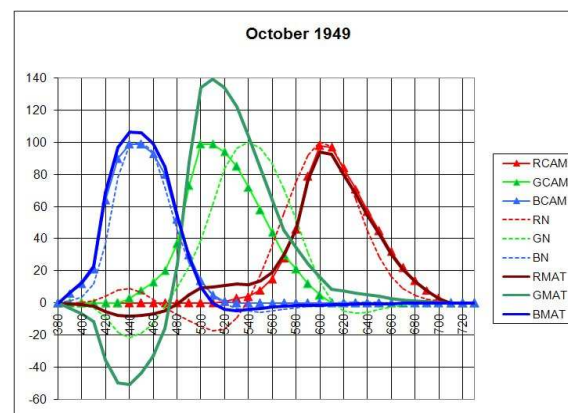


Figure 61. October 1949 taking characteristics

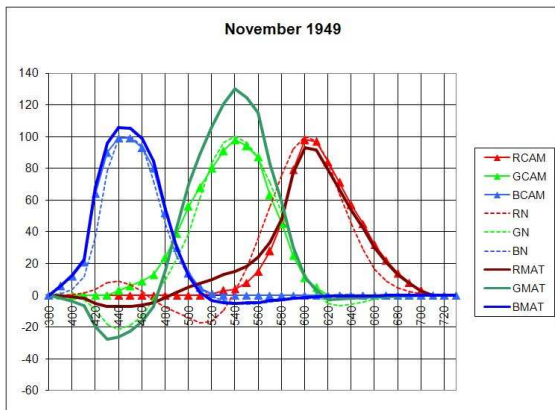


Figure 62. November 1949 taking characteristics

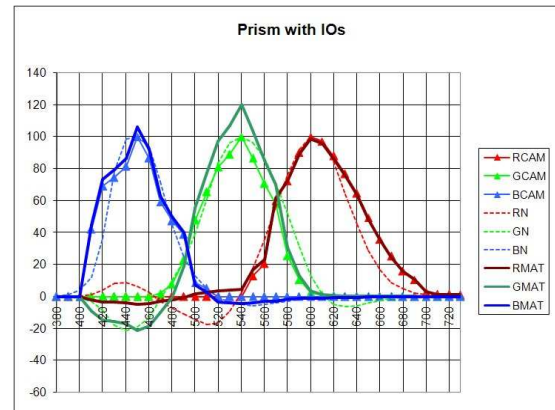


Figure 65. Prism camera taking characteristics

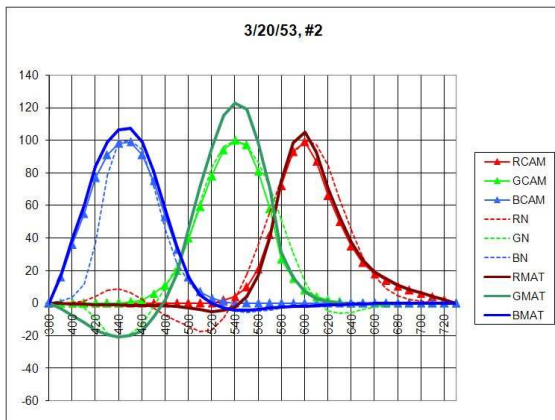


Figure 63. March 1953 Camera no. 2 taking characteristics

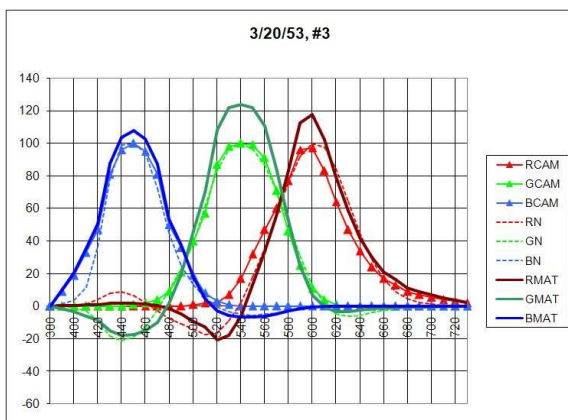


Figure 64. March 1953 camera no.3 taking characteristics

Figure 57 shows the ideal taking characteristics for the NTSC primaries. Figure 61 through Figure 65 show the characteristics for various cameras for which data is available. These latter figures each show three sets of curves: RCAM, GCAM and BCAM (lighter color with data point symbols) represent the raw spectral sensitivities of the camera. RN, GN, BN (thinner and lighter color dashed lines) are the standard NTSC characteristics (also shown on a different scale in Figure 57). RMat, GMat, BMat (darker lines without symbols) represent matrixed characteristics calculated by the least-squares fit to the correct test chart colors

Curves of individual components such as the prism optics [Ref16] and the image orthicon response [Ref17] were inserted into a spreadsheet graph as a background picture and the spreadsheet values were then adjusted manually until the plotted curve matched the background.

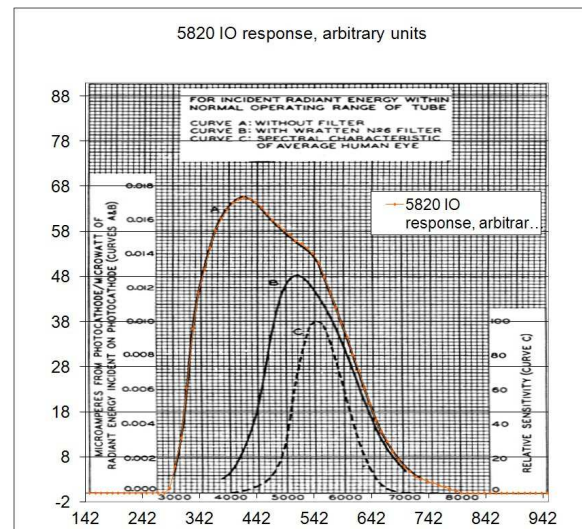


Figure 66. Tracing of image orthicon spectral sensitivity curve

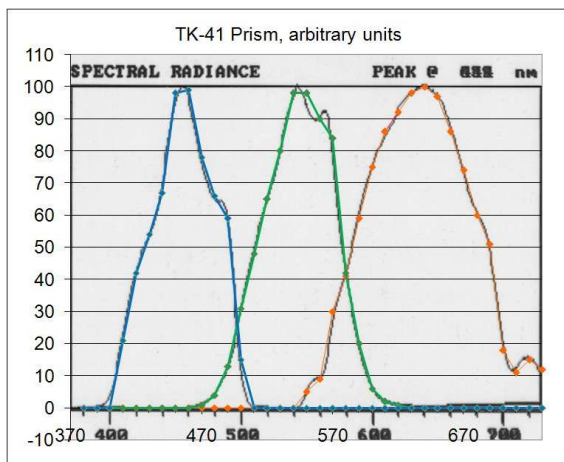


Figure 67. Prism measurements as provided, with 10-nm interval tracings

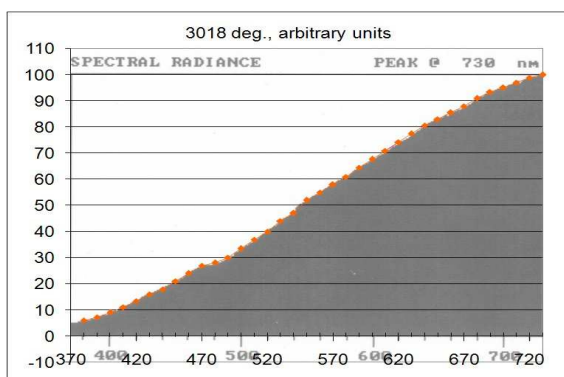


Figure 68. 3018 K illumination used to obtain prism curves

The instrument used to measure the prism optics provided curves normalized to a peak value of 100 (Figure 67), but did not compensate for the source illumination. This was measured separately (Figure 68) and traced in a spreadsheet. The data in Figure 67 was then divided point-by-point by the data from Figure 68 and renormalized to obtain the data for Figure 65.

Transmission percentages of trimming filters were obtained directly from tables in [Ref18]. Any effects due to non-flatness of neutral density filters used to balance the RGB signal levels were ignored. Some types of neutral density filters exhibit increased attenuation at the short wavelengths (400 -440 nm), possibly affecting the blue channel if used there [Ref18].

The author was not able to obtain spectra for the test objects used in [Ref04] or [Ref12]. The calculations therefore used the SMPTE 303M color chart [Ref19]. This chart also has the advantage that the colors generally fall within the gamut of

modern monitors, so the results can be displayed without distortion. Averaged user-measured spectra for the commercial version of the chart are published on the internet [Ref20]. Additional test object spectra recommended for use in specifying camera performance are given in [Ref31] and [Ref32] but are not used in this study. Further related information on camera, telecine, and monitor characteristics is found in [Ref29] through [Ref36].

8.1.5 Stage-By-Stage Optics Analysis

A second spreadsheet was developed for the cases where the spectral curves of individual components were known. This spreadsheet does the wavelength-by-wavelength calculation of the over-all response of the RGB channels, which can then be transferred to the first spreadsheet for color rendition calculations of the color chart.

An analysis was carried out using the dichroic filter examples given in [Ref21]. These results indicate that Widdop's example filters were not used in cameras for which we have data. In particular, Widdop's filters appear to have more and/or different passband ripple than appears in actual cameras.

Widdop's mirror transmittances are given as graphs in [11]. Mirror reflectance was calculated as (1-transmittance).

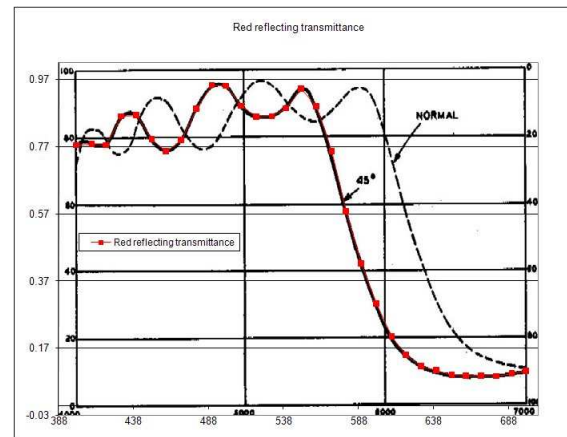


Figure 69. Tracing of Widdop's red mirror transmittance

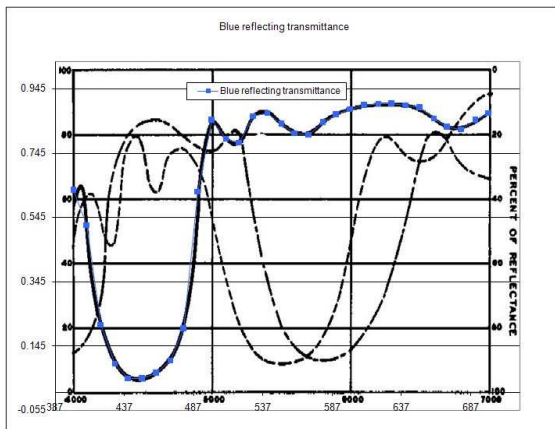


Figure 70. Tracing of Widdop's blue mirror transmittance

8.1.5.1 Red channel per Widdop

The stages in the red channel are the blue mirror transmittance, the red mirror reflectance, two trimming filters, and the image orthicon.

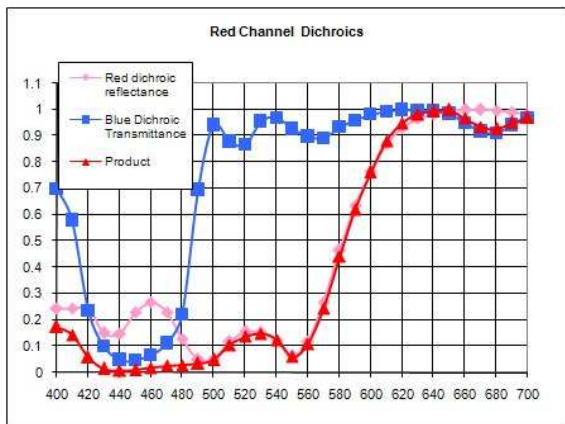


Figure 71. Red channel dichroic mirrors

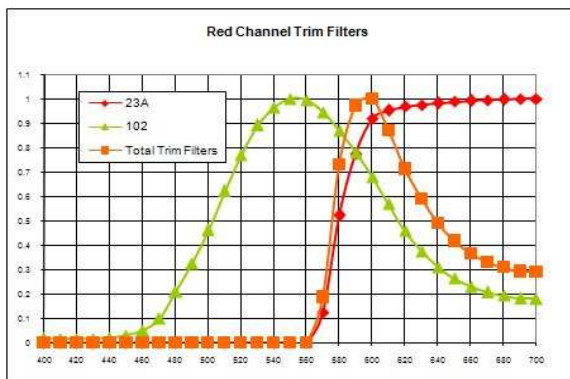


Figure 72. Red channel trimming filters

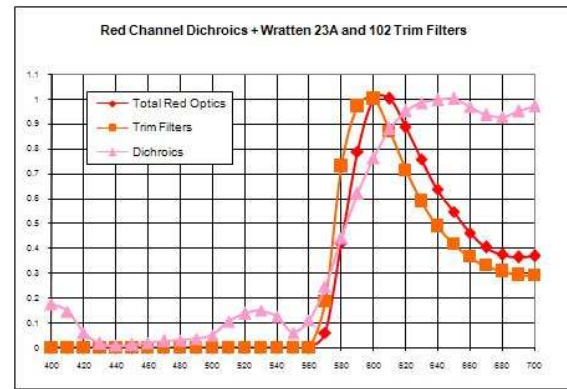


Figure 73. Red channel dichroics plus trimming filters

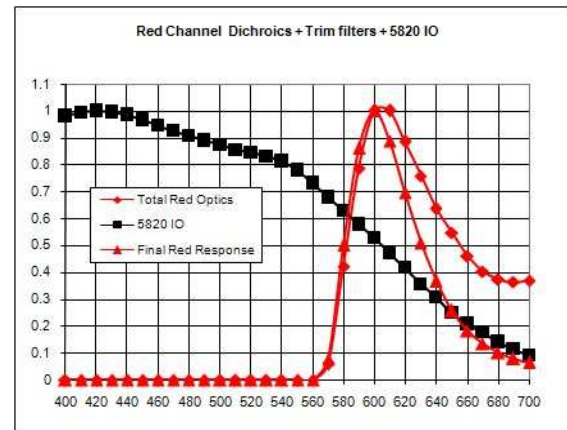


Figure 74. Red channel optics plus image orthicon

8.1.5.2 Green channel per Widdop

The stages in the green channel are the red and blue mirror transmittances, a trimming filter, and the image orthicon.

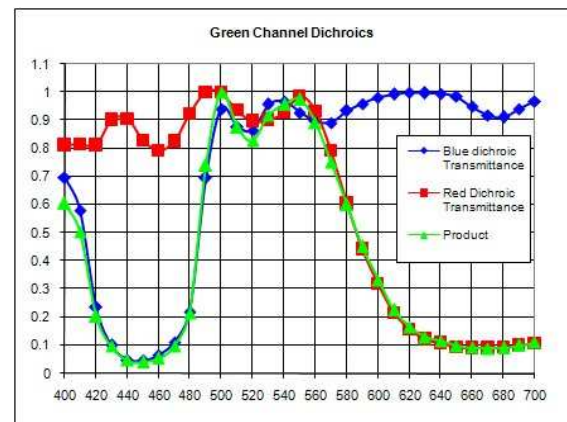


Figure 75. Green channel dichroic mirrors

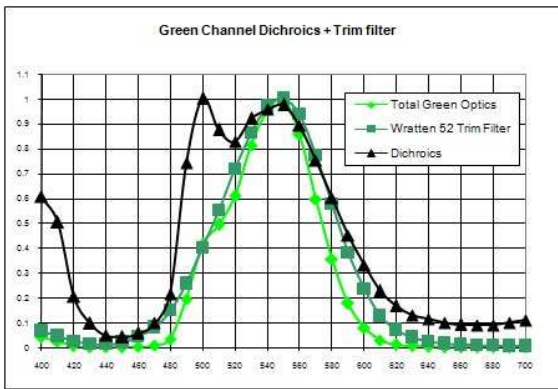


Figure 76. Green channel dichroic mirrors plus trimming filter

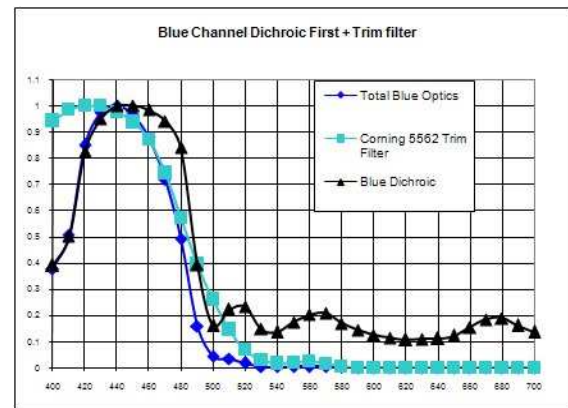


Figure 79. Blue channel dichroic mirror plus trimming filter

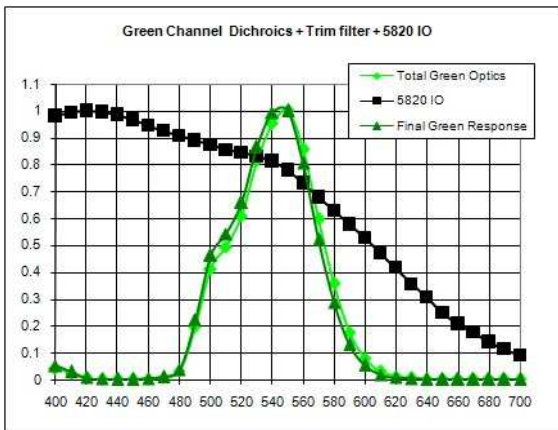


Figure 77. Green channel optics plus image orthicon

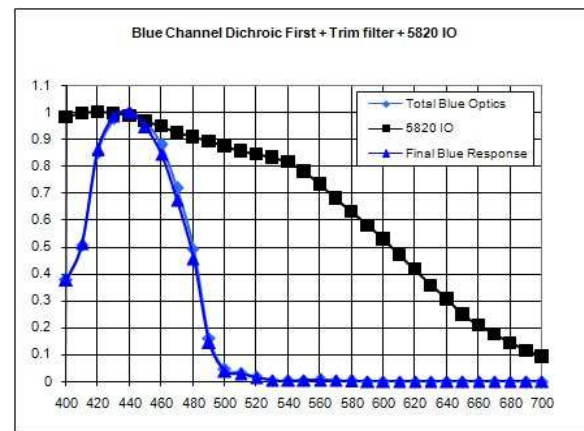


Figure 80. Blue channel optics plus image orthicon

8.1.5.3 Blue channel per Widdop

The stages in the blue channel are the blue mirror reflectance, a trimming filter, and the image orthicon.

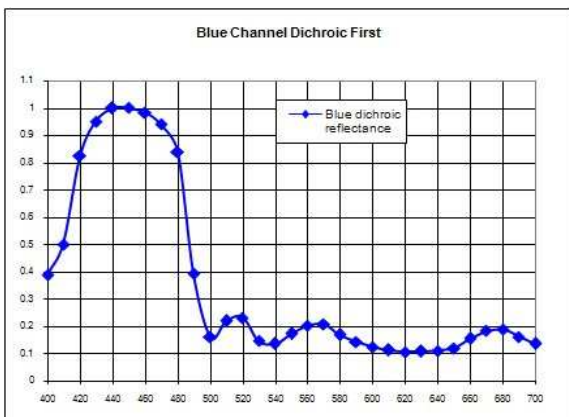


Figure 78. Blue channel dichroic mirror

8.1.5.4 Over-All Result With Widdop's Mirrors

Figure 81 shows the over-all result of multiplying the various attenuation factors in each color channel. Figure 82 shows the same results normalized to a peak of 1.0. The green channel in particular is less smooth than any of the measured camera data that we have, indicating that dichroic mirrors with less transmission ripple were used in practical cameras.

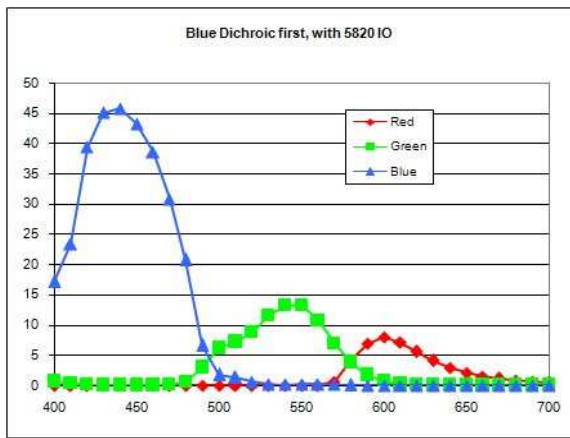


Figure 81. Over-all results with Widdop's mirrors

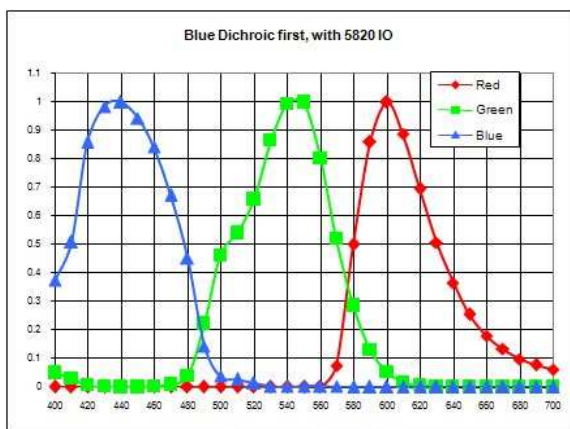


Figure 82. Over-all results normalized to 1.0

8.1.6 Calculation Methods

In accordance with the published data, calculations involving spectra were made by numerical integration at 10 nm intervals from 380 nm to 730 nm. The use of 10 nm intervals can result in small errors that were deemed to be insignificant compared to the over-all errors in camera response.

In order to not over-emphasize the effects of neutral objects on the least-squares fit, the five gray and black patches were excluded from the calculations. The least squares fit thus depended on 19 of the 24 patches.

A program internal to the spreadsheet was written that would present a display representing the color chart with its square color patches each divided into three vertically adjacent rectangles. The ideal original color is displayed in the center rectangle. The color is shown as reproduced with a particular camera and display in the top rectangle. The color as reproduced with the same camera and display including a

least-squares matrix is in the bottom rectangle. Copying this display from the screen to the computer clipboard allowed importing it into other programs for further manipulation or publication.

The calculations include corrections for display gamma and re-matrixing to the proper values for display on a sRGB monitor [Ref10, Ref11]. For the purposes of this work, the sRGB primaries were used ($x_R = 0.64$, $y_R = 0.33$, $x_G = 0.30$, $y_G = 0.60$, $x_B = 0.15$, $y_B = 0.06$ in the CIE 1931 system), but the gamma curve was set to a constant exponent of 2.2, which is easily realized in the image processing program.

As part of the matrix calculations, the image could be adjusted to show a change in white point between Illuminant C (the original NTSC specification) and D65 (the sRGB white point). Usually, no adjustment was made, in order to keep white point shift from being confused with errors due to the camera's non-ideal spectral response, which is the main focus of this study.

Colors errors were plotted on both the 1931 CIE chromaticity chart with horizontal and vertical axes representing the dimensionless quantities x and y respectively (for example, Figure 84) and the 1976 uniform chromaticity scale (UCS) chart with horizontal and vertical axes u' and v' respectively (for example, Figure 85) [Ref22].

9 Results for NTSC displays

The following figures show the outputs of the spreadsheet calculations. In the color charts, each color patch has a central third representing the ideal reproduction (the original patch), an upper third showing the raw camera response, and a lower third showing the result of the experimental least-squares matrix.

The CIE and UCS charts show the chromaticities of the color patches. Cyan symbols represent the original color; black the raw camera output; and orange the matrixed output. The UCS diagrams also show a dot representing the approximate just-noticeable difference in chromaticity, and a circle representing the approximate extremes of color differences expected from variations in normal color vision. The reader is reminded that the chromaticity charts do not show differences in brightness, which are sometimes of the same order of magnitude as the chromaticity differences.



Figure 83 October 1949 camera



Figure 86. November 1949 camera

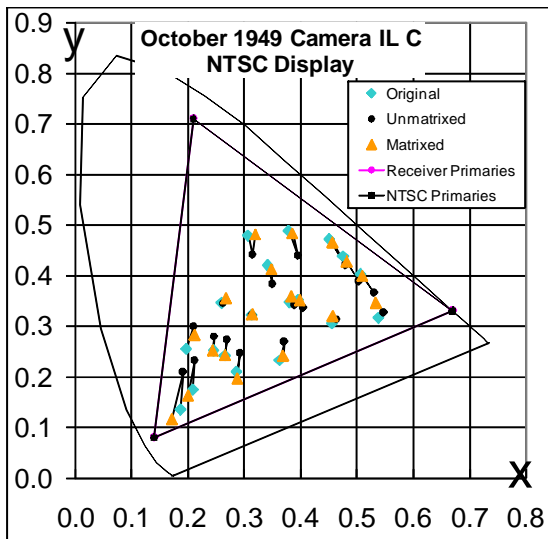


Figure 84. October 1949 camera CIE chart

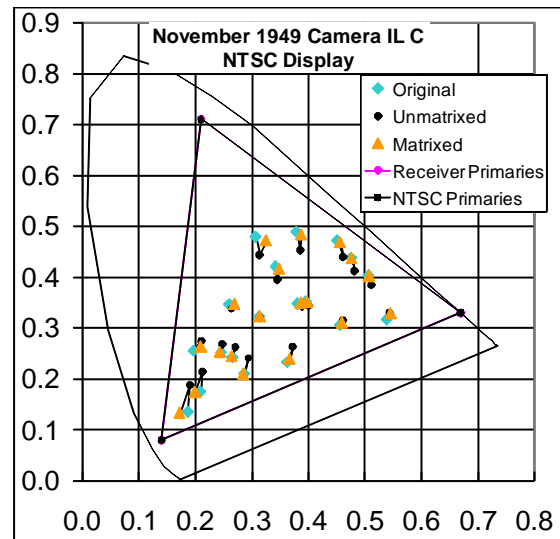


Figure 87. November 1949 camera CIE chart

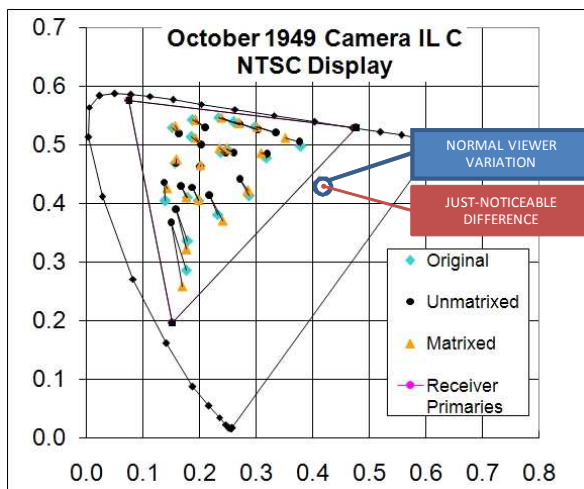


Figure 85. October 1949 camera UCS chart

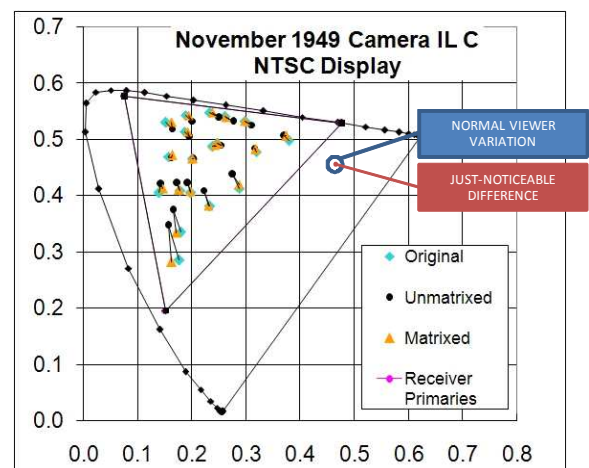


Figure 88. November 1949 camera UCS chart



Figure 89. March 1953 no.2 camera



Figure 92. March 1953 no.3 camera

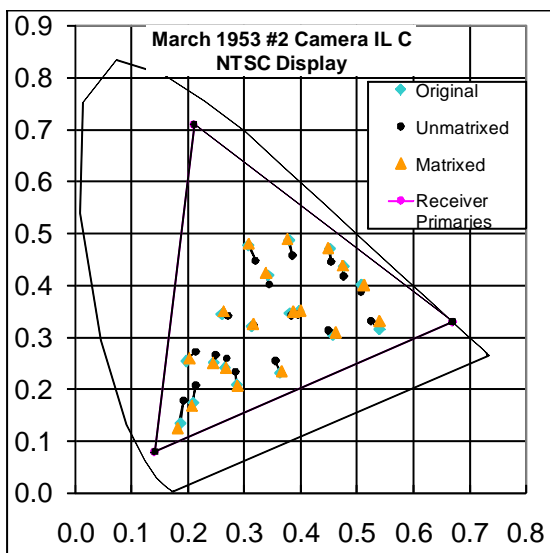


Figure 90. March 1953 no.2 camera CIE chart

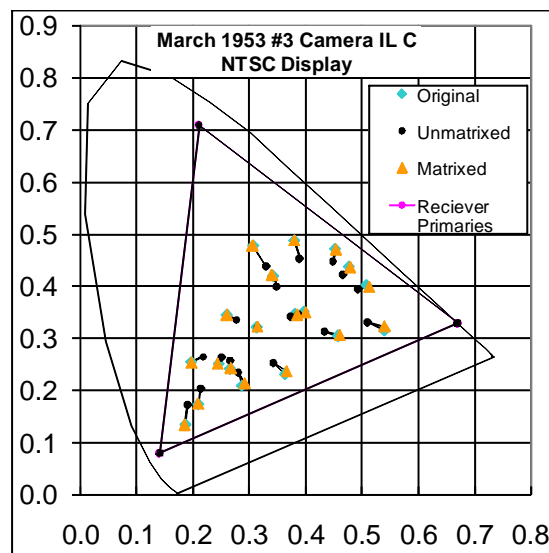


Figure 93. March 1953 no.3 camera CIE chart

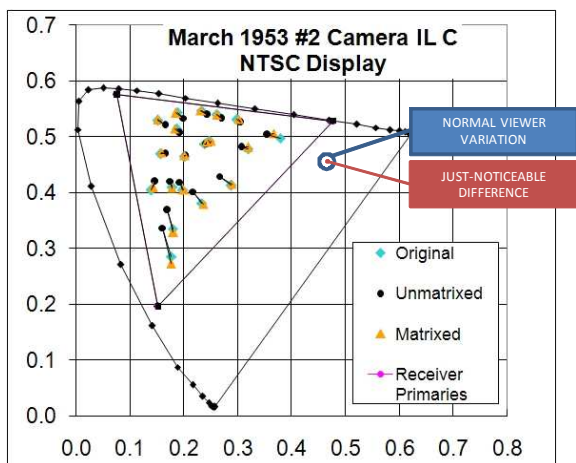


Figure 91. March 1953 no.2 camera UCS chart

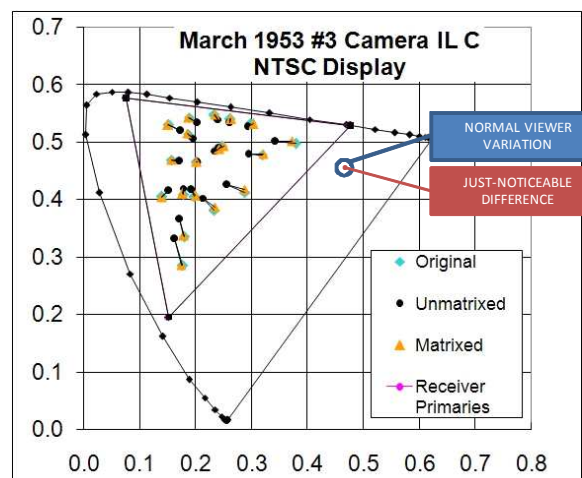


Figure 94. March 1953 no.3 camera UCS chart



Figure 95. Prism camera

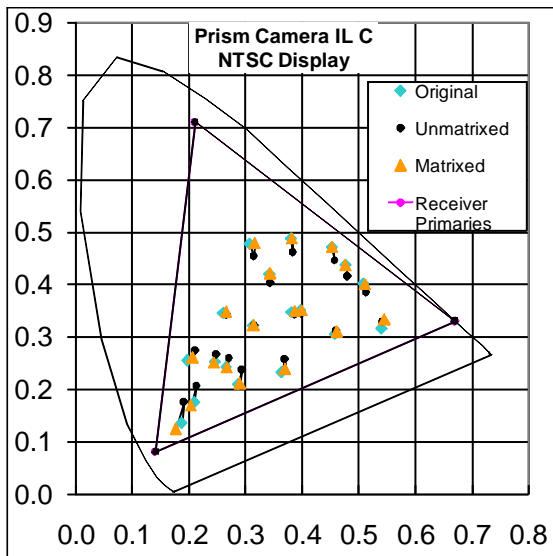


Figure 96. Prism camera CIE chart

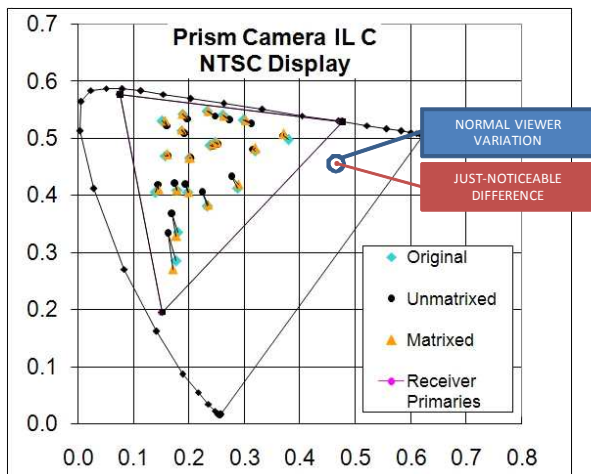


Figure 97. Prism camera UCS chart

10 Linear Luminance Curves

The linear luma charts show the luminance spectral response ignoring the fact that pure spectral colors are outside the camera gamut. These give a fair representation of the luminance reproduction compared to the ideal, if it could be assumed that luminance is calculated before the RGB signals are clipped at black. They are a good representation of the relative contributions of all wavelengths for colors that are inside the gamut. However, the curves will change depending on gain adjustments of the RGB channel gains to match a particular illuminant.

Each chart shows the raw camera curve YCAM, the standard luminance curve YN, and the matrixed camera curve YMAT.

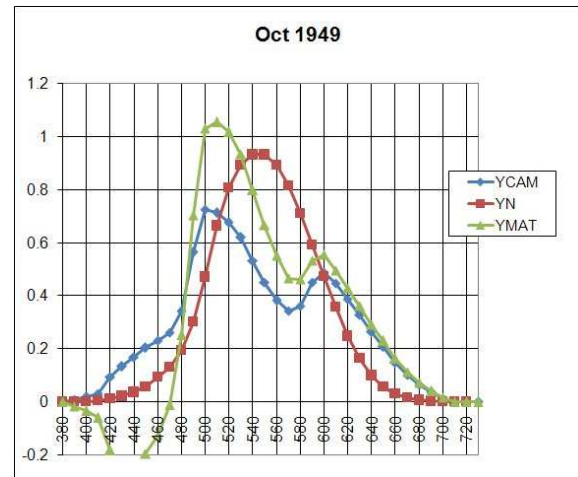


Figure 98. October 1949 linear luma

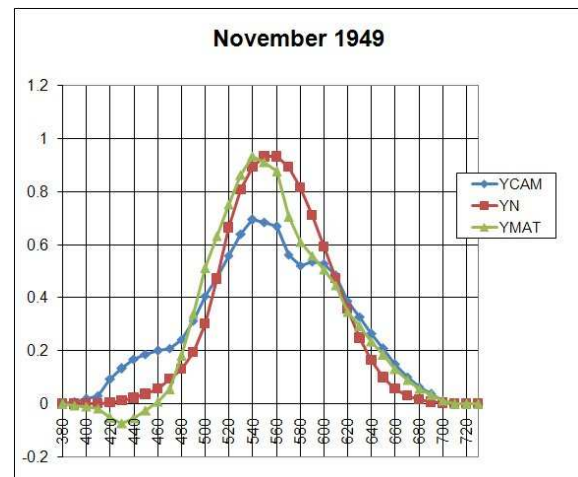


Figure 99. November 1949 linear luma

11 Results for Experimental and Hypothetical Displays

11.1 Trinoscope

The trinoscope display in [Ref04] had a somewhat more saturated and less-yellow green than the eventual NTSC green. Its blue primary was also considerably more violet than NTSC blue. It was quite a close match to the March 1953 camera no.2. The trinoscope red is practically identical to the ideal NTSC red.

11.2 Reduced-Gamut Display

A hypothetical reduced-gamut display was also studied in [Ref04]. It appears that after the theoretical spectral sensitivities were calculated and graphed in [Ref04], this line of investigation was abandoned, probably because the large negative lobe required implied that results would be unacceptable without a correction matrix. The NTSC primaries have the advantage of needing small negative lobes. The effect of small negative lobes can be approximated for most object spectra simply by using narrowed versions of the positive lobes.

It is a simple matter to plug the reduced-gamut primary chromaticities into the spreadsheet and calculate a corrective matrix. The results with the reduced-gamut display are shown below. In this case, the linear least squares matrix performs very poorly, as it pushes the colors to the edge of the small gamut and brightens them excessively. Some other compromise would be required to get acceptable results with this hypothetical display.



Figure 103. March 1953 camera no. 2 with trinoscope display (illuminant C scene lighting)

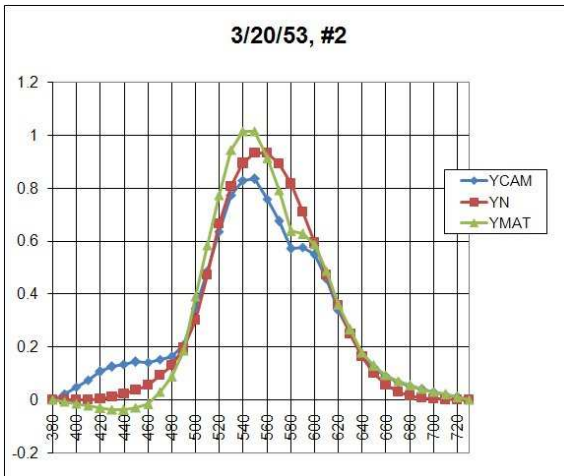


Figure 100. March 1953 no.2 linear luma

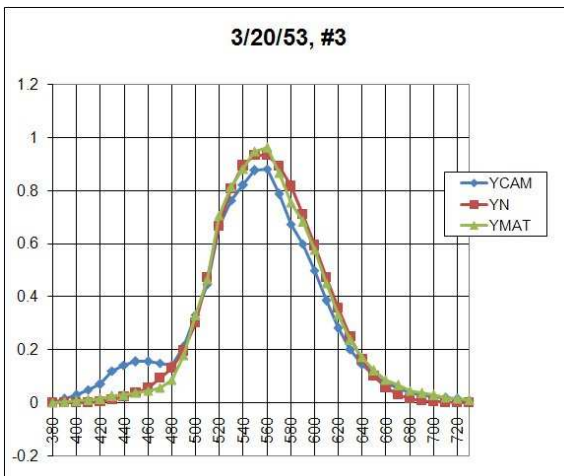


Figure 101. March 1953 no.2 linear luma

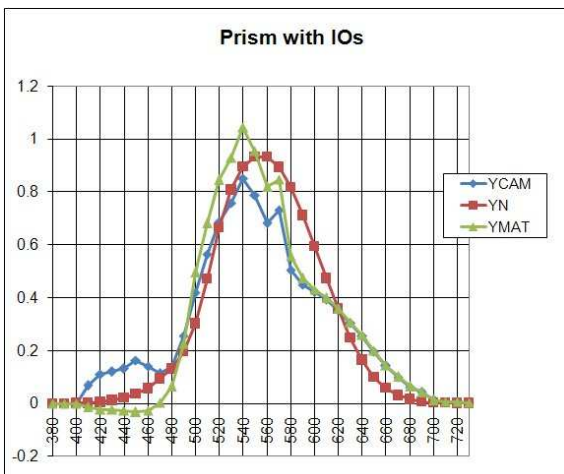


Figure 102. Prism linear luma

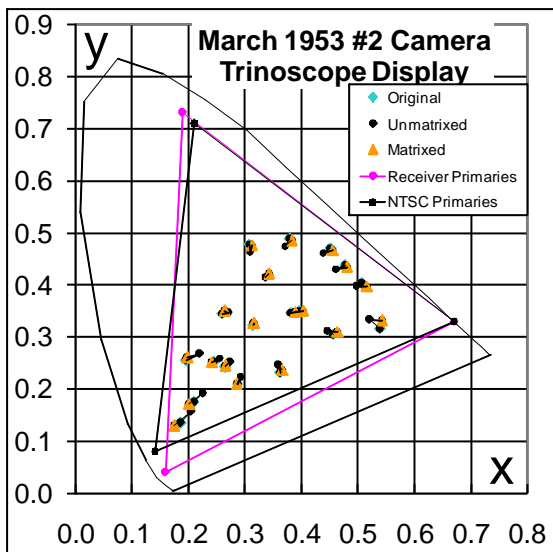


Figure 104. March 1953 camera no. 2 with trinoscope display (illuminant C scene lighting) CIE chart

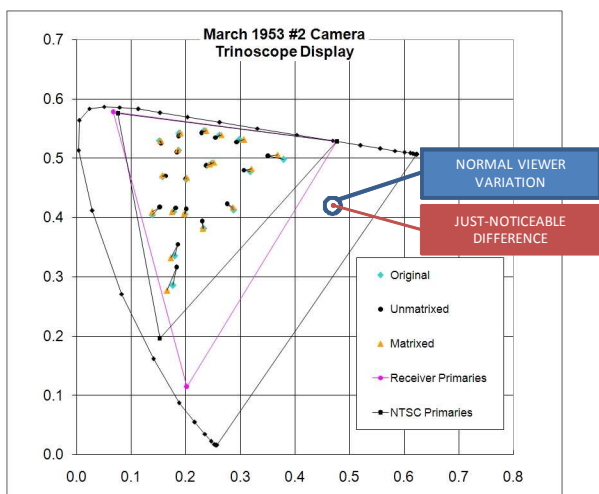


Figure 105. March 1953 camera no. 2 with trinoscope display (illuminant C scene lighting) UCS chart



Figure 106. March 1953 camera no. 2 with small-gamut display (illuminant C scene lighting)

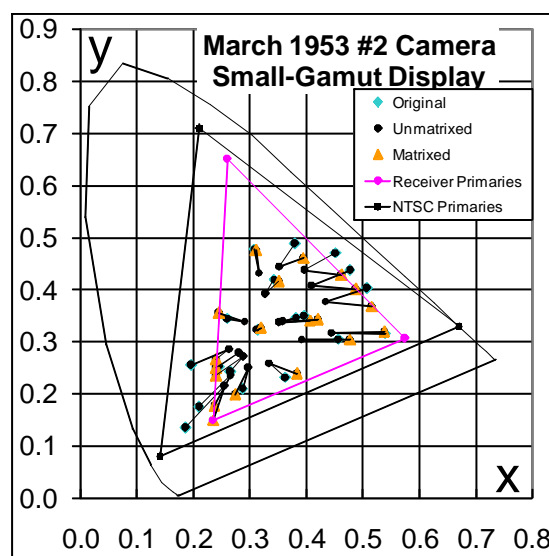


Figure 107. March 1953 camera no. 2 with small-gamut display (illuminant C scene lighting) CIE chart

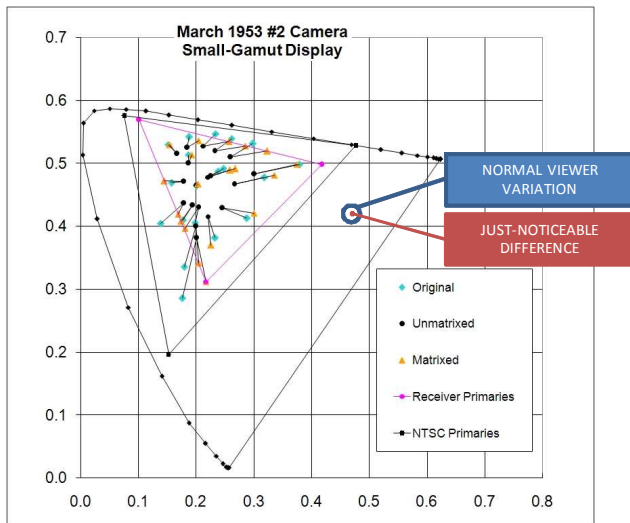


Figure 108. March 1953 camera no. 2 with small-gamut display (illuminant C scene lighting) UCS chart

12 Approximate Results for Images

12.1 Calculation Method

For these calculations, the object spectra are unknown. Therefore, the input image is assumed to be the correct version and the possible effects of any unusual reflectance spectra are ignored.

A first attempt to simulate the camera effects was made by using the inverse of the linear least-squares correction matrix. However, examination of the results above will show that the matrix does not correct all the colors on the chart perfectly. Therefore, the inverse matrix will also have imperfections in representing the effects of the camera on the original scene. A better alternative is to use the hue and saturation adjustments in an image processing program that allows separate adjustment of the major primary and secondary hues. In this case, the adjustments are made to the “ideal” center parts of the color patches to make them as close as possible to the computed raw camera output. The resulting adjustment parameters are saved as an adjustment layer that can then be applied to a complete image to obtain an approximation of the raw camera output.

The image processing layers are shown in Figure 109. The input images are in the sRGB color space, and include gamma correction, as is typically the case for digital still images. The process layers consist of:

- Linearization by applying a gamma adjustment
- Matrixing from sRGB primaries to the NTSC color space,
- Hue , saturation and lightness adjustment as determined beforehand to match a particular camera,
- Matrixing to sRGB color space
- Application of gamma correction
- Application of a text label

The resultant image is viewable on an sRGB monitor.

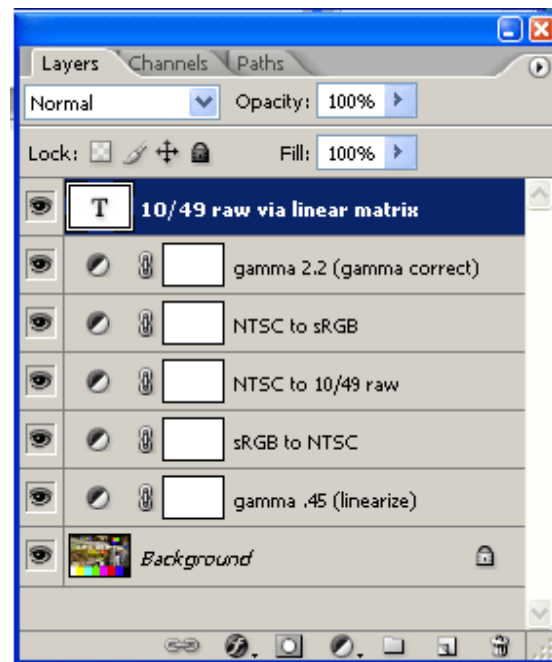


Figure 109. Layers for inverse matrix process

12.2 Example Images



Figure 110. Veggie Market original [copyright Wayne E. Bretl]



Figure 111. Veggie Market as seen by 10/49 camera under IL C



Figure 112. Veggie Market as seen by Prism camera under IL A

13 Incandescent Lighting

Although the analysis of the TK-41 colorimetry is simplified by assuming the scene is illuminated by daylight, the camera was most often used under incandescent studio lighting. We know that the white balance was adjusted to a first approximation by insertion of neutral density filters into two of the red, green and blue channels, rather than by use of color compensating filters in the main optical path. This means that the taking characteristics of the camera actually changed due to the tilt in the incandescent light spectrum (Figure 49). Some analysis was done on the shift in camera taking curves and the resulting color reproduction.

Figure 113 shows the NTSC taking characteristics multiplied by Illuminant C (dotted curves RNC, GNC, BNC) and Illuminant A (solid curves RNA, RNA, RNA). These curves have been normalized for equal area, that is the camera has been white balanced. Besides the change in crossover points of the curves, there is a notable change in the amplitudes of the minor lobes of each curve when the illuminant is changed.

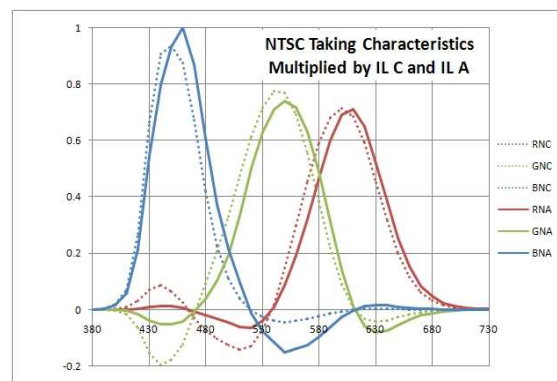


Figure 113 NTSC taking curves multiplied by IL C (dotted) and IL A (solid)

Figure 114 and Figure 115 show the results of the illuminant change for the March 1953 no. 3 camera and the prism camera, respectively. The NTSC curves multiplied by illuminant C, which is the standard condition, are included as dotted lines for comparison.

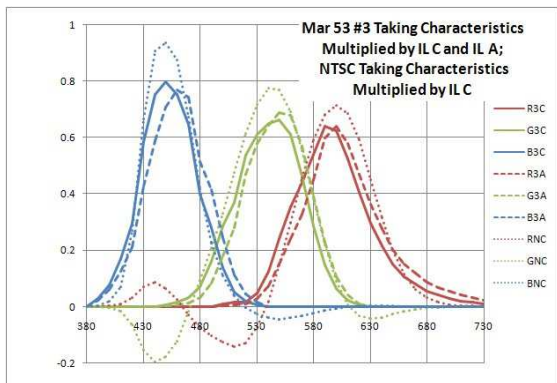


Figure 114 March 1953 camera no.3 taking curves multiplied by IL C (solid) and IL A (dashed). Dotted lines: NTSC multiplied by IL C

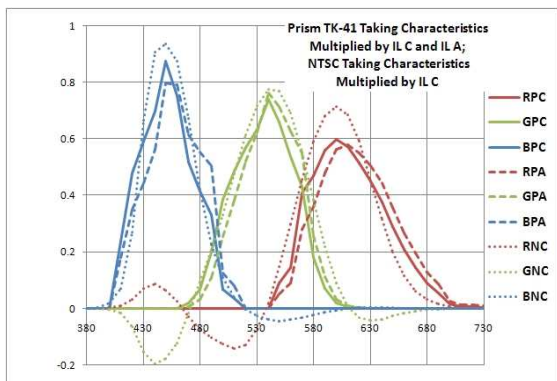


Figure 115 Prism camera taking curves multiplied by IL C (solid) and IL A (dashed). Dotted lines: NTSC multiplied by IL C

Figure 116 through Figure 118 show the comparison of the responses to illuminants C and A for the March 1953 camera number 3.

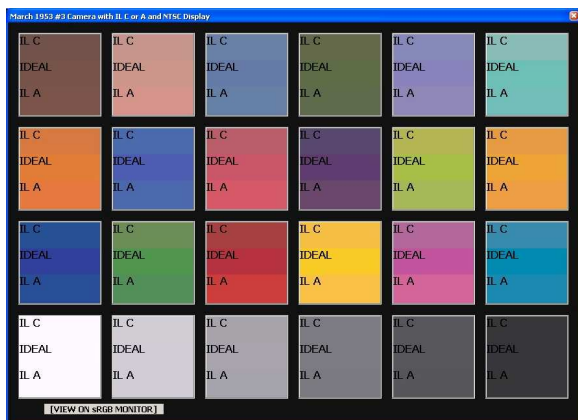


Figure 116 March 1953 camera under illuminants C and A

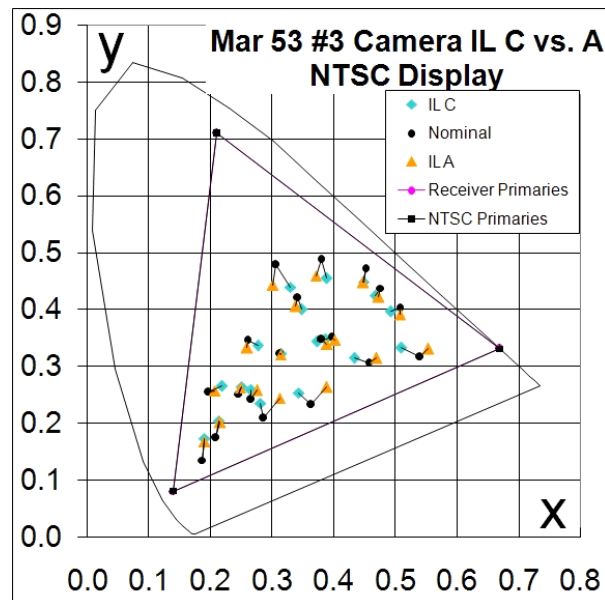


Figure 117 March 1953 camera #3 under illuminants C and A

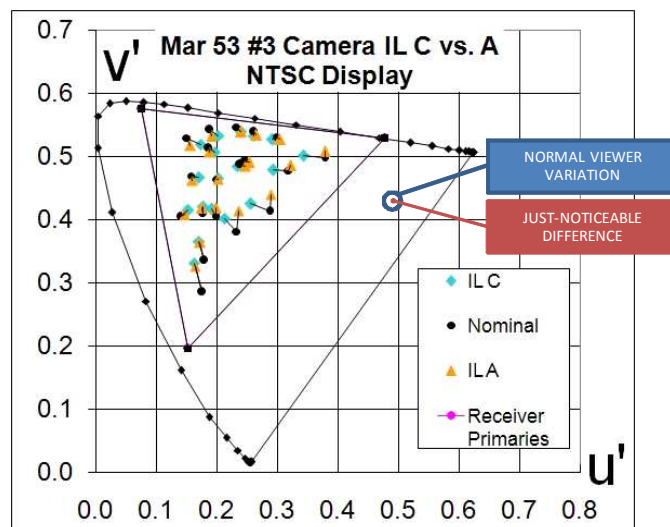


Figure 118 March 1953 camera #3 under illuminants C and A

Figure 119 through Figure 121 show the performance of the no.3 camera of March 1953 under incandescent lighting. These should be compared with the figures showing this camera under Illuminant C. Some colors show opposite distortions, for example the red and magenta patches are too dark under Illuminant C and too bright under Illuminant A. The least squares matrix shows some unusual over-correction in the case of Illuminant A, and this matrix would have to be modified for practical use.



Figure 119 March 1953 camera no.3 under Illuminant A

Figure 125 through Figure 127 show similar calculations for the prism camera. Again, the least squares matrix seems to be over-correcting.



Figure 122 Prism camera under illuminants C and A

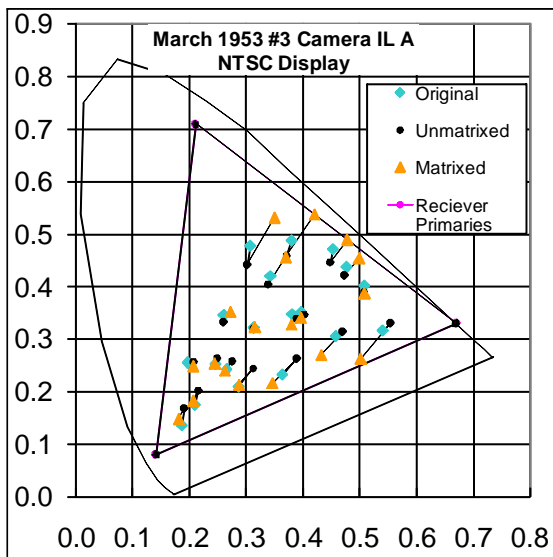


Figure 120. March 1953 camera no.3 under Illuminant A

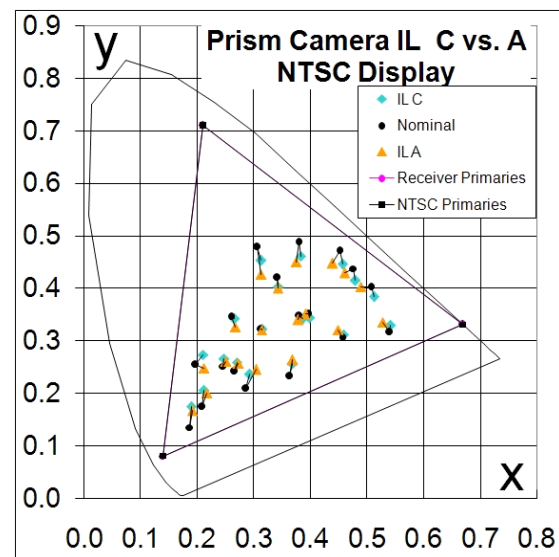


Figure 123 Prism camera under illuminants C and A

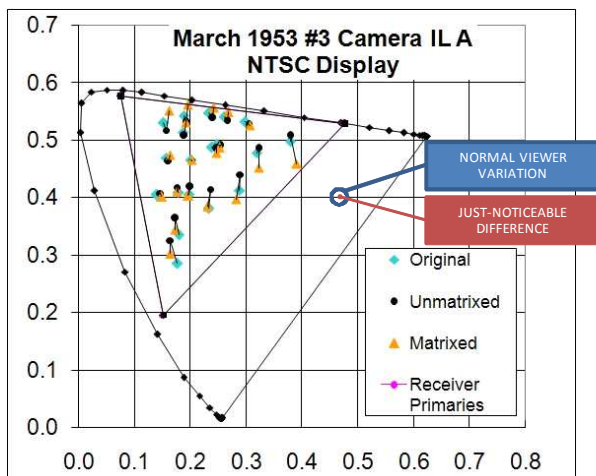


Figure 121. March 1953 camera no.3 under Illuminant A

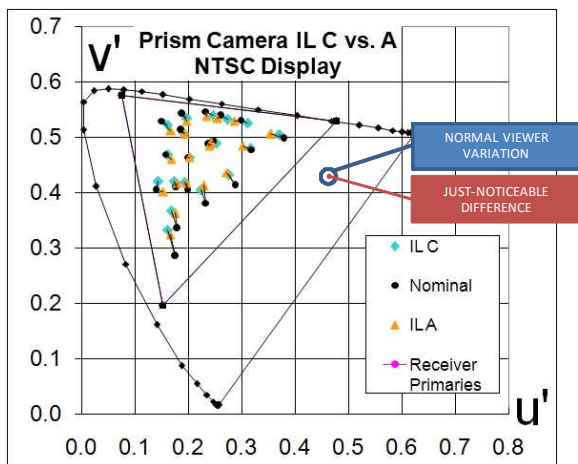


Figure 124 Prism camera under illuminants C and A

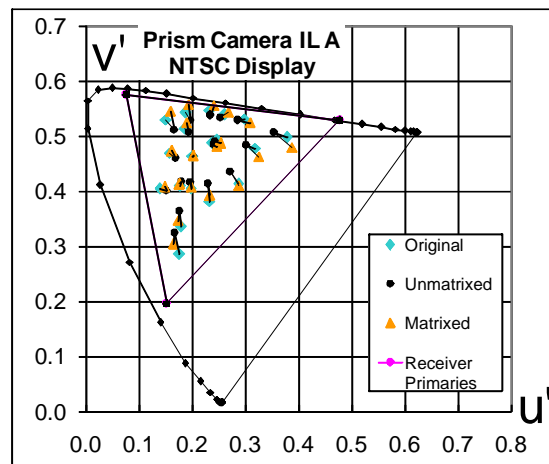


Figure 127. Prism camera under Illuminant A UCS chart



Figure 125. Prism camera under Illuminant A

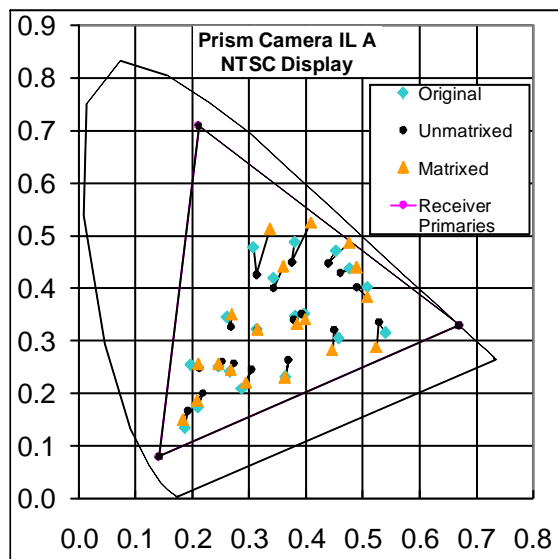


Figure 126. Prism camera under Illuminant A CIE chart

14 Conclusions

Extensive spectral calculations were done on the basis of historical data measured on early image orthicon cameras. The exact results that would be obtained with these cameras and a color test chart were determined by spectral calculations in a spreadsheet, and presented in CIE and UCS diagrams. A program was also written to display the results properly on a modern monitor for direct viewing. Furthermore, approximate effects of these cameras on real scene images were simulated using the results of the spreadsheet programs in an image processing program.

Analysis of the data available indicates that the TK-41 color analysis optics were close to optimum for an un-matrixed camera feeding an NTSC display. Complaints of incorrect color (except for the green hair problem caused by polarization effects) must be attributed to other factors involving instabilities in the electronic systems following the optics. It can be concluded that restored video tapes of early programs should be good representations of the original program sets and costumes, subject to any variations in camera setup and operation

15 Acknowledgements

The author wishes to thank the following people for supplying information, advice, and leads to old documents. The author specifically wants to thank Jay Ballard for making the measurements of the TK-41C prism assembly.

Jay Adrick

Jay Ballard

Pete Deksnis

Erich Loepke

Wayne Luplow

Ed Reitan

16 References

[Ref01] Jay Adrick, private communication, 2007

[Ref02] TV Display Phosphors/Primaries – Some History, LeRoy DeMarsh, Journal SMPTE, December 1993

[Ref03] Cathode-Ray-Tube Phosphors: Principles and Applications, Simon Larach and Austin E. Hardy, Proceedings of the IEEE, Vol. 61, No.7, July 1973

[Ref04] Before the Federal Communications Commission, Washington D.C., Petition of Radio Corporation of America and National Broadcasting Company, Inc. for Approval of Color Standards for the RCA Color Television System, June 25, 1953

[Ref05] Optical System Diagram for MI-40534 Color Camera, <http://home.att.net/~pldexas/potpourri2/lastpage6.html>

[Ref06] Color Television Engineering, John W. Wentworth, McGraw-Hill Book Company, Inc., 1955, pp.292-293

[Ref07] The Reproduction of Colour, Third Ed., R.W. G. Hunt, Fountain Press, 1975

[Ref08] Color Science, 2nd Ed, G. Wyszecki and W.S. Stiles, John Wiley & Sons, 1982

[Ref09] Color Television, Selections from the Journal of the SMPTE, Richard S. O'Brien, Ed., Society of Motion Picture and Television Engineers, 1970

[Ref10] IEC 61966-2-1 Multimedia systems and equipment - Colour measurement and management - Part 2-1: Colour management - Default RGB colour space – sRGB

[Ref11] ITU-R BT.709-5, Parameter values for the HDTV standards for production and international programme exchange

[Ref12] Optimum Color Analysis Characteristics and Matrices for Color Television Cameras with Three Receptors, A. H. Jones, Journal SMPTE, Vol. 77, February 1968

[Ref13] Colour Error Reduction in Video Systems, R.J. Green and S.J. Ismail, IEEE Transactions on Broadcasting, Vol. 36 No. 1, March 1990

[Ref14] NTIA Technical Memorandum TM-04-406, Color Correction Matrix for Digital Still and Video Imaging

Systems, Stephen Wolf, U.S. DEPARTMENT OF COMMERCE, December 2003

[Ref15] Spectral Response of Color Cameras, I. Bosonoff and W. J. Derenbecher, Radio Corporation of America, April 10, 1953

[Ref16] Measurements of TK-41C camera prism assembly, Jay Ballard [private communication, 2007]

[Ref17] 5820 Image Orthicon (specification data sheets), Tube Division, Radio Corporation of America, Harrison, New Jersey (5820 -10-56), also similar data sheets for image orthicons type 5826, 6474, and 7037

[Ref18] Handbook of Chemistry and Physics, 69th Ed., 1988 1989, CRC Press, Inc., "Transmission of Corning Colored Filters" and "Transmission of Wratten Filters", pp. E-406 to E-420

[Ref19] SMPTE Standard 0303M-2002, Television – Color Reference Pattern

[Ref20] http://www.babelcolor.com/main_level/ColorChecker.htm#How_about_data

[Ref21] Review of Work on Dichroic Mirrors and Their Light-Dividing Characteristics, Mary Ellen Widdop, Journal SMPTE, Vol. 60, April 1953

[Ref22] Measuring Colour, R.W.G. Hunt, Halsted Press Div. of John Wiley & Sons, 1987

[Ref23] The Performance Characteristics of Yttrium Oxyphosphide – A New Red Phosphor for Color Television, Austin E. Hardy, IEEE Transactions on Electron Devices, Vol ED-15, No. 11, November 1968

[Ref24] <http://www.color.org/sRGB.xalter>

[Ref25] Television Receiver White Color: A Comparison of Picture Quality with White References of 9300 K and D6500 Zwick, D.M.; [Broadcast and Television Receivers, IEEE Transactions on](#), Volume BTR-19, [Issue 4](#), Nov. 1973 pp. 205 – 213

[Ref26] A Second Generation Color Tube Providing More Than Twice the Brightness and Improved Contrast Fiore, J.P.; Kaplan, S.H.; [Broadcast and Television Receivers, IEEE Transactions on](#), Volume BTR-15, [Issue 3](#), Oct. 1969 pp. 267 – 276

[Ref27] Computing Colorimetric Errors of a Color Television Display System

Neal, C.B.; [Consumer Electronics, IEEE Transactions on](#), Volume CE-21, [Issue 1](#), Feb. 1975 pp. 63 – 73

[Ref28] An Analysis of the Necessary Decoder Corrections for Color Receiver Operation with Non-Standard Receiver Primaries

Parker, N. W.; IEEE Transactions on Broadcast and Television Receivers, Volume BTR-12 No.1, April 1966; Reprinted in [Consumer Electronics, IEEE Transactions on](#), Volume CE-28, [Issue 1](#), Feb. 1982 pp. 74 – 83

Note: [Ref29 –Ref36] can be found at http://www.ebu.ch/en/technical/publications/tech3000_series/index.php

[Ref29] t3213 EBU Standard for Chromaticity Tolerances for Studio Monitors - first edition 1975

[Ref30] t3218 Colour Telecines, Methods of Measurement and Specifications - third edition 1988

[Ref31] t3237 Methods of Measurement of the Colorimetric Fidelity of Television Cameras - first edition 1983

[Ref32] t3237-s1 Methods of Measurement of the Colorimetric Fidelity of Television Cameras - Supplement 1, Measurement Procedures - second edition 1989

[Ref33] t3238 Methods of Measuring the Main Characteristics of Television Cameras - first edition 1983

[Ref34] t3263 Specification of Grade-1 Colour Picture Monitors - second edition (editorial corrections 2006)

[Ref35] t3273 Methods of Measurement of the Colorimetric Performance of Studio Monitors - first edition 1993

[Ref36] t3320 User requirements for Video Monitors in Television Production 2007

[Ref37] Colorimetric Performance of Non-Standard Television Receiver with Customer Adjustment
Bretl, W.E., Consumer Electronics, IEEE Transactions on, Volume CE-25, Issue 1, Feb. 1979 pp. 100 – 110
[mistakenly listed as “Breti” in some indexes]

[Ref 38] Broadcast Camera Equipment for Monochrome and Color Television, Radio Corporation of America, Broadcast and Television Equipment Division, Camden, NJ, 1956

[Ref 39] Color Television Theory, Equipment, Operation: Manual for Television Technical Training, Second Edition, 1959, Radio Corporation of America

[Ref40] RCA Photosensitive Devices and Cathode-Ray Tubes, Form No. CRPD-105A, 1958, Radio Corporation of America

[Ref41] Image Orthicons for Color Cameras, R. G. Neuhauser and A. A. Rotow, Proc. IRE, Vol 42 No.1, January 1954, pp. 161-165

[Ref42] A Study of the Need for Color Controls on Color TV Receivers in a Color TV System Operating Perfectly, Charles J. Hirsch, IEEE Transactions on Broadcast and Television Receivers, Nov. 1964, pp. 71-96